

Accepted Manuscript

Design and synthesis of selective CYP1B1 inhibitor *via* dearomatization of α -naphthoflavone

Makoto Kubo, Keiko Yamamoto, Toshimasa Itoh

PII: S0968-0896(18)31894-7
DOI: <https://doi.org/10.1016/j.bmc.2018.11.045>
Reference: BMC 14649

To appear in: *Bioorganic & Medicinal Chemistry*

Received Date: 9 November 2018
Revised Date: 29 November 2018
Accepted Date: 29 November 2018

Please cite this article as: Kubo, M., Yamamoto, K., Itoh, T., Design and synthesis of selective CYP1B1 inhibitor *via* dearomatization of α -naphthoflavone, *Bioorganic & Medicinal Chemistry* (2018), doi: <https://doi.org/10.1016/j.bmc.2018.11.045>

This is a PDF file of an unedited manuscript that has been accepted for publication. As a service to our customers we are providing this early version of the manuscript. The manuscript will undergo copyediting, typesetting, and review of the resulting proof before it is published in its final form. Please note that during the production process errors may be discovered which could affect the content, and all legal disclaimers that apply to the journal pertain.



Design and synthesis of selective CYP1B1 inhibitor *via* dearomatization of α -naphthoflavone.

Makoto Kubo, Keiko Yamamoto, Toshimasa Itoh*

Laboratory of Drug Design and Medicinal Chemistry, Showa Pharmaceutical University, 3-3165

Higashi-Tamagawagakuen, Machida, Tokyo 194-8543, Japan

*Corresponding author

Toshimasa Itoh: titoh@ac.shoyaku.ac.jp; phone, +81 42 721 1581; Fax, +81 42 721 1580

Abstract

Selective cytochrome P450 (CYP) 1B1 inhibition has potential as an anticancer strategy that is unrepresented in the current clinical arena. For development of a selective inhibitor, we focused on the complexity caused by sp^3 -hybridized carbons and synthesized a series of benzo[*h*]chromone derivatives linked to a non-aromatic B-ring using α -naphthoflavone (ANF) as the lead compound. Ring structure comparison suggested compound **37** as a suitable cyclohexyl-core with improved solubility. Structural evolution of **37** produced the azide-containing *cis*-**49a**, which had good properties in three important respects: (1) selectivity for CYP1B1 over CYP1A1 and CYP1A2 (120-times and 150-times, respectively), (2) greater inhibitory potency of more than 2 times that of ANF, and (3) improved solubility. The corresponding aromatic B-ring compound **59a** showed low selectivity and poor solubility. To elucidate the binding mode, we performed X-ray crystal structure analysis, which revealed the interaction mode and explained the subtype selectivity of *cis*-**49a**.

1. Introduction

Cytochromes P450 (CYPs) constitute a superfamily of heme-containing enzymes capable of catalyzing oxidative biotransformations of both endogenous and exogenous compounds such as steroidal hormones, bile acids, various kinds of xenobiotics and drugs, and therefore are important for biological drug discovery.¹⁻⁴ The CYP1 family, CYP1B1, CYP1A1 and CYP1A2, notably concerns the bioactivation of procarcinogenic compounds.⁵⁻⁸ Polycyclic aromatic hydrocarbons (e.g., benzo[*a*]pyrene and 7,12-dimethylbenz[*a*]anthracene) are representative CYP1 family substrates.⁹⁻¹² These are procarcinogens, which are activated by the CYP1 family. Hence, the CYP1 family has been recognized as a target for chemoprevention against these carcinogens.^{5,6}

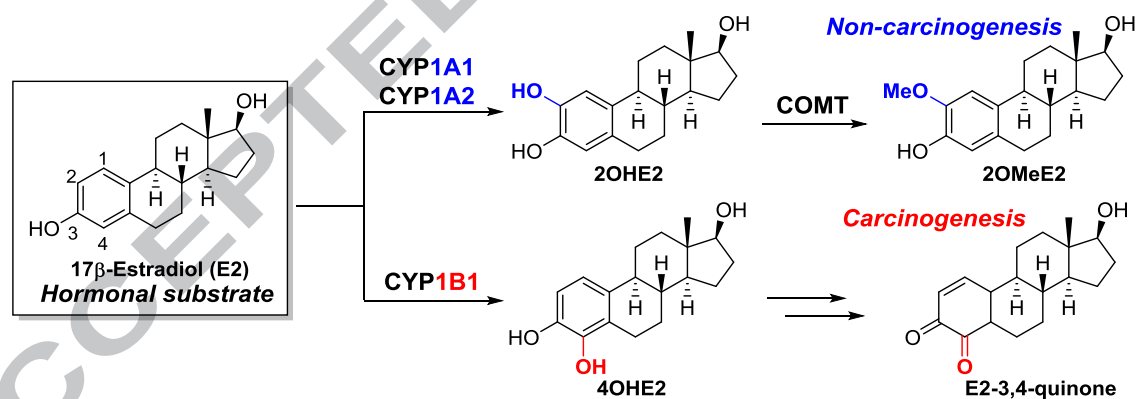


Figure 1. Metabolic pathways of 17β-estradiol (E2) catalyzed by CYP1A1, CYP1A2 and CYP1B1. CYP1 family and catechol-*O*-methyltransferase (COMT) are responsible for the E2 metabolism. 2-Hydroxylation of the E2 regulated by the CYP1A1/1A2 affords 2-hydroxy-estradiol (2OHE₂), and which is then methylated by COMT to produce 2-methoxy-estradiol (2OMeE₂). CYP1B1 affords 4-hydroxy-estradiol, and which is gradually oxidized to estradiol-3,4-quinone (E2-3,4-quinone).

The CYP1 family also plays an important role in the metabolism of endogenous estrogens,¹³⁻¹⁵ 17 β -estradiol (E2) and estrone (E1), which cause estrogen-dependent cancers¹⁶ such as breast cancer and ovarian cancer (Figure 1). 2-Hydroxylation of E2 regulated by CYP1A1 and CYP1A2 has been recognized as a major inactivation pathway of E2, which affords 2-hydroxy-E2 (2OHE₂) as a metabolite,^{14,17} and methylation by catechol-O-methyltransferase (COMT) affords an inactivated metabolite.¹⁸ On the other hand, CYP1B1 produces 4-hydroxy-E2 (4OHE₂).¹⁹ In contrast to 2OHE₂, 4OHE₂ retains strong estrogenic activity^{17,20} and is gradually oxidized to quinone compounds,^{21,22} which are tumor initiators, because they are easily converted to oxidized products with resistance to COMT-mediated inactivation.¹⁸ The major metabolite of E2 is 2OHE₂ in normal human tissues, but in some tumor tissues, there are high levels of 4OHE₂ owing to over-expression of CYP1B1.^{23,24} For these reasons, 4-hydroxylation by CYP1B1 has been recognized as a mechanism of carcinogenesis. Moreover, CYP1B1 is involved in the metabolism of some anticancer agents²⁵⁻²⁷ (e.g., Docetaxel, Tamoxifen and Flutamide) used for the treatment of hormonal cancers and is thought to cause drug resistance. These reports indicate that selective CYP1B1 inhibition could be an anticancer strategy unrepresented in the current clinical arena.

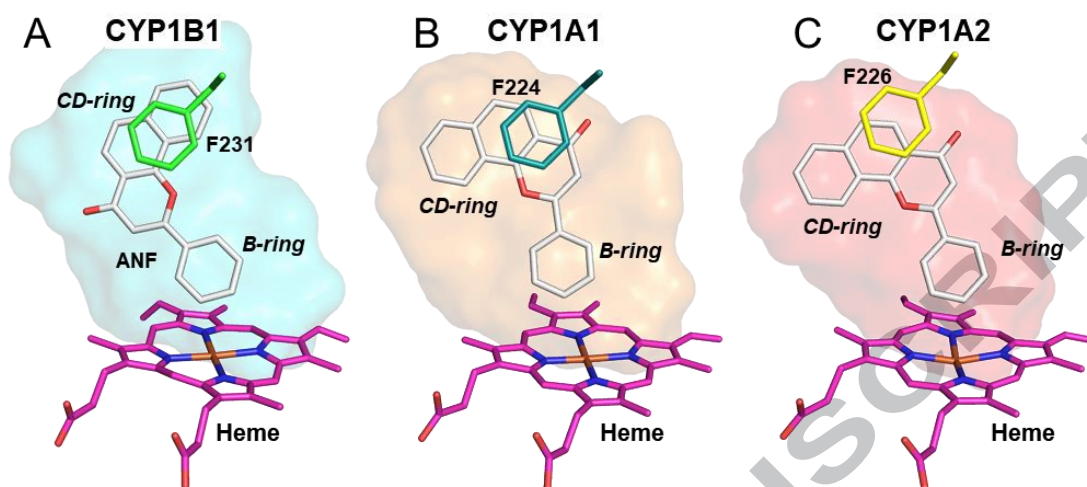


Figure 2. Binding mode of ANF in CYP1B1 (green) (A) (PDB: 3PM0²⁸), CYP1A1 (teal) (B) (PDB:4I8V²⁹) and CYP1A2 (yellow) (C) (PDB: 2HI4³⁰). ANF (white), heme (magenta) and residues are presented as stick models in atom type. Cavities of CYP1B1, CYP1A1 and CYP1A2 were calculated with Surflex Dock program³¹ on Sybyl X2 (Tripos) and shown in cyan, orange and red, respectively. The orientations of ANF are opposite between CYP1B1 and CYP1A1/1A2. ANF has a π - π stacking interaction with a conserved phenylalanine in CYP1 family. The position of B-ring is near the heme.

Crystal structures of hCYP1A2, 1A1 and 1B1 have been reported in holo form with *a*-naphthoflavone (ANF) as an inhibitor (Figure 2).^{28–30} Homology of the sequences of the active sites is high among the CYP1 family members, and thus the environments of the substrate-binding sites are similar and are composed of planar substrate-binding cavities. Several classes of CYP1 inhibitors have been reported, including flavonoids, *trans*-stilbenes, coumarins, and alkaloids.^{5–7} In particular, the structural evolution of ANF, a representative non-selective CYP1 inhibitor, produced the strongest CYP1B1 inhibitor.³² However, ANF derivatives and some other types of inhibitors have a disadvantage in that their aqueous solubility is low owing to their rigid and planar structures created by the sp^2 carbon atoms.³³

Solubility is an important physical property in drug development.³⁴ Ishikawa and co-workers successfully improved the solubility by a new concept,^{33,35} i.e., planarity-disruption by introduction of *ortho*-substituents in a β -naphthoflavone.³⁶ For the design of selective CYP1B1 inhibitors, we focused on sp^3 -hybridized carbons for two-reasons: (1) high fraction sp^3 (F_{sp^3}) compounds have more potential as drugs due to their increased complexity, which is expected to reduce promiscuity³⁷ and increase solubility,³⁸ (2) the effect on selectivity and inhibitory potency of the 3-dimensional (3D) property has not been investigated in the design of CYP1B1 inhibitors. Despite the planar CYP1 cavities, the 3D design could possibly bind by an induced fit strategy because the environment around the heme is formed by a flexible loop structure. For these reasons, we planned to design ANF-based CYP1B1 inhibitors having sp^3 carbons to improve the selectivity among the CYP1 family and increase the aqueous solubility.

Herein, we report the development of dearomatized ANF derivatives designed for selective CYP1B1 inhibition activity and improvement of solubility. To verify our strategy, we synthesized these inhibitors as well as aromatic reference compounds, and measured their ethoxyresorufin-*O*-deethylase (EROD) activities and solubilities in PBS. In addition, to evaluate the binding mode, we characterized hCYP1B1 spectroscopically in the presence of an inhibitor and performed the co-crystallization of the hCYP1B1 and inhibitor.

2. Results and discussion

2.1. Design of CYP1B1 Inhibitor

To improve the selectivity and solubility, we attempted to increase the complexity of ANF by conversion of the sp^2 carbons into sp^3 carbons. ANF binds to the CYP1 family but the CD-ring is oriented in the opposite direction between CYP1B1 and CYP1A1/1A2 (Figure 2). In the active site of the CYP1B1, the CD-ring has a critical π - π stacking interaction with Phe231 conserved in the CYP1 family and the B-ring is oriented toward the heme. We selected the B-ring as a dearomatization site based on this binding mode. Initially, we planned to find a suitable sp^3 -ring and then optimize it by adding substituents containing oxygen, sulfur and nitrogen atoms (Figure 3).

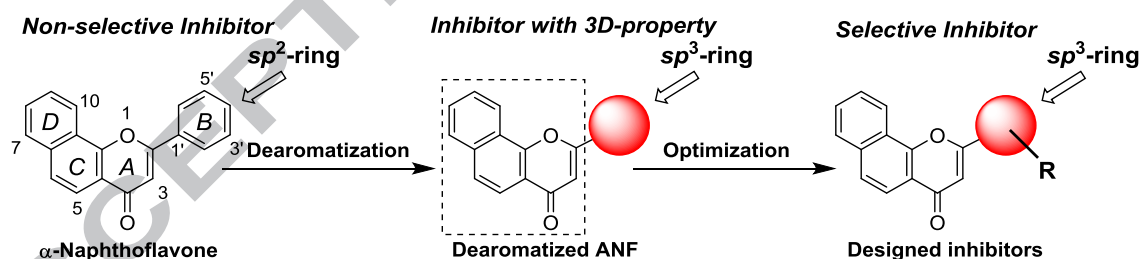
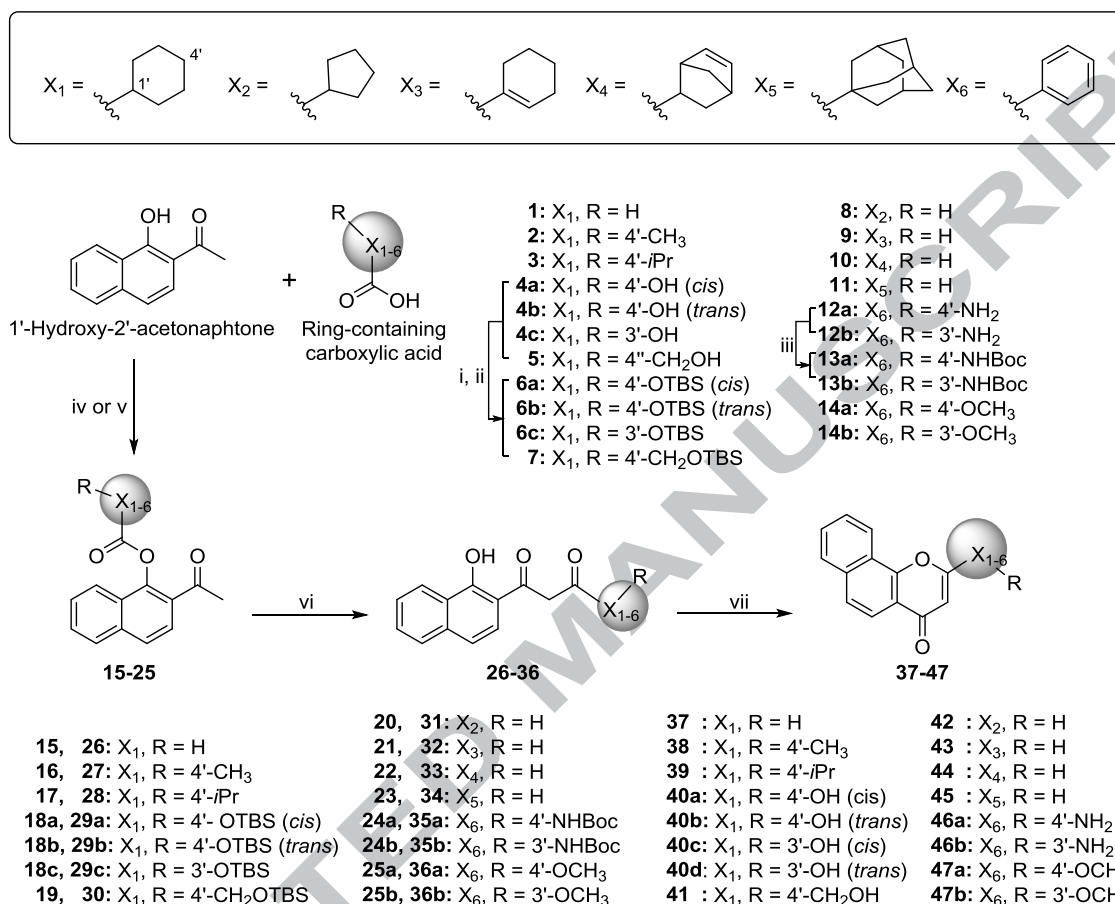


Figure 3. Our strategy for selective CYP1B1 inhibitor. Chemical Structures of ANF and design inhibitors containing benzo[*h*]chromone skeleton (middle structure, *dash line*) are shown. Partial numbering of carbons and ANF (A-D) ring identification (left structure) are reported. First stage of our strategy is dearomatization of ANF to find suitable sp^3 -ring (*red sphere*) against CYP1B1, and second stage is optimization of substitute groups.

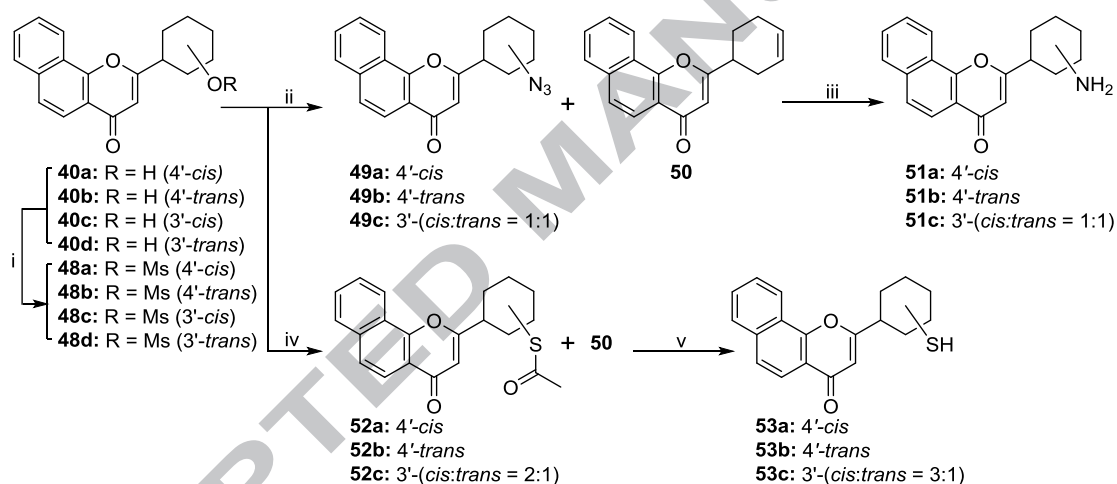
2.2. Chemical Synthesis



Scheme 1. Synthetic routes for Benzo[*h*]chromone Derivatives. Reagents and conditions: (i) TBSCl, Et₃N, DMF, rt; (ii) NaOH, MeOH/THF, rt; (iii) (Boc)₂O, Et₃N, 1,4-dioxane/H₂O, rt; (iv) SOCl₂, pyridine, DCM, rt; (v) DCC, DMAP, DCM, rt; (vi) *t*-BuOK, THF, rt; (vii) conc. H₂SO₄, EtOH, 80 °C.

Benzo[*h*]chromone derivatives containing various B-ring structures **37-47** with cyclohexyl, cyclopentyl, norbornyl, adamantyl or phenyl moieties were synthesized using 1'-hydroxy-2'-acetonaphthone as a starting material (Scheme 1). Carboxylic acids **1-3**, **8-11**, and **14** were esterified by the Shotten-Baumann reaction with 1'-hydroxy-2'-acetonaphthone. In the case of **6a-c**, unintended deprotection occurred, thus after prepared of silyl- or *t*-Boc-protected **6a-c**, **7**, and **13a,b** from **4a-c**, **5**,

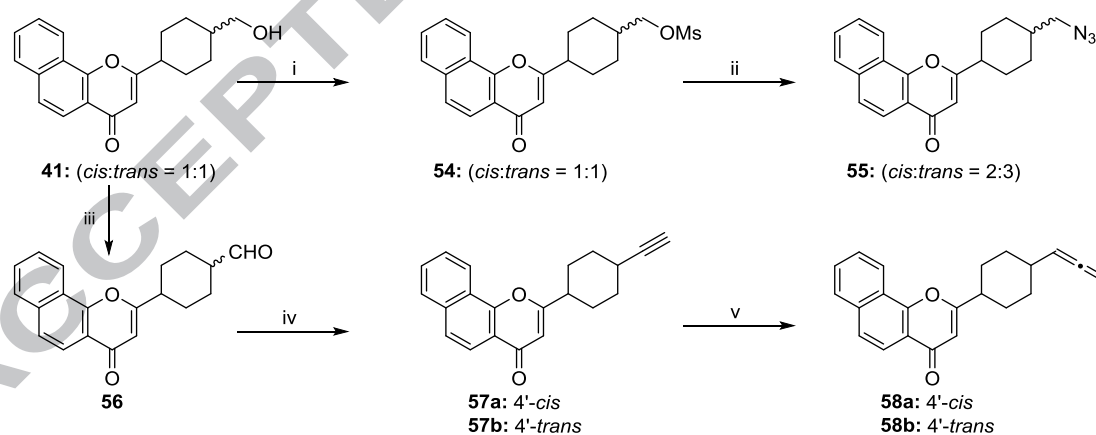
and **12a,b**, these were reacted by Steglich esterification to give the corresponding esters **18a-c**, **19** and **24a,b**, respectively. Subsequently, Baker-Venkataraman rearrangement^{39,40} of esters **15-25** with potassium *tert*-butoxide provided 1,3-diketones **26-36**, which were then cyclized by removal of the silyl and *t*-Boc protecting groups using sulfuric acid to give the desired benzo[*h*]chromone derivatives **37-47**.



Scheme 2. Synthesis of Cyclohexane Derivatives. Reagents and conditions: (i) MsCl, Et₃N, DCM, rt; (ii) NaN₃, DMF, 80 °C; (iii) NaBH₄, NiCl₂·6H₂O, MeOH/THF, 0 °C; (iv) AcSH, K₂CO₃, DMF, 80 °C; (v) K₂CO₃, THF/MeOH, 0 °C.

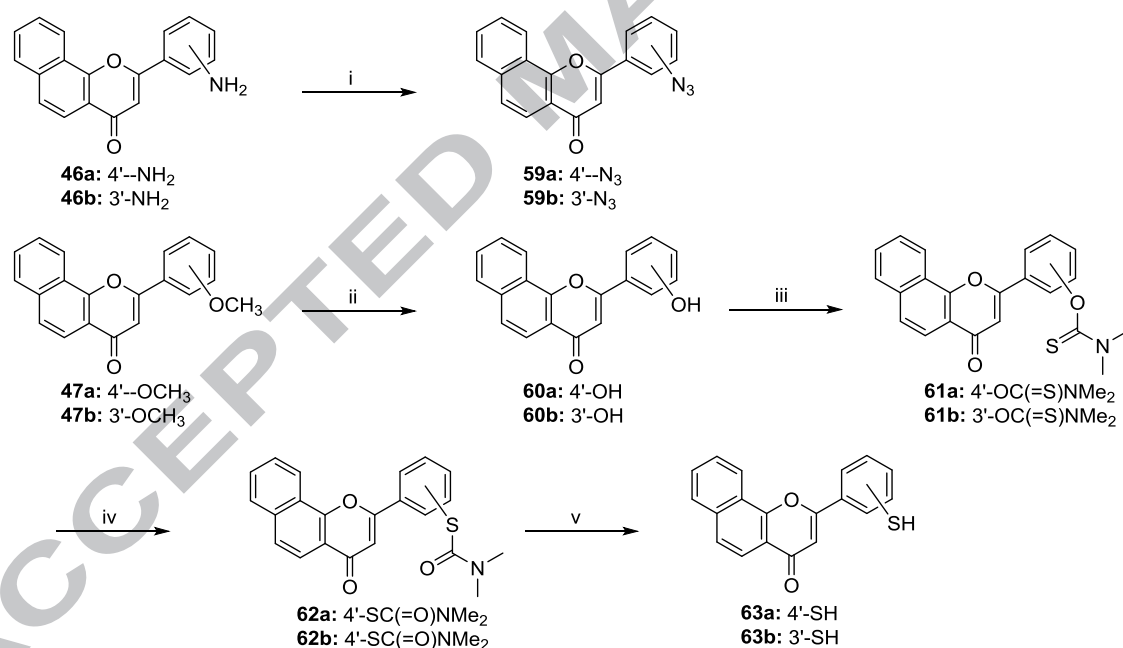
In order to screen the substituents, we synthesized cyclohexane derivatives (Scheme 2). Four cyclohexanol isomers **40a-d** containing regioisomers and geometrical isomers were converted to mesylates **48a-d**, respectively. 4'-*trans*-Mesylate **48b** was treated with sodium azide in *N,N*-dimethylformamide (DMF) at 80 °C to give *cis*-azide **49a** together with *trans*-azide **49b** and 3-cyclohexene **50**, which was formed by elimination of the methanesulfonyl substituent, in low

selectivity. To improve the selectivity, we varied the conditions such as reagent equivalents, temperature, leaving groups and the counterpart *trans*-isomer **48b**. Nevertheless, there were no conditions that gave our desired selectivity. As a result, **49a,b** were separated by MPLC, and the other isomer **49c** was obtained as a diastereomixture (*cis:trans* = 1:1). Synthesis of amines **51a-c** was carried out using sodium borohydride in the presence of nickel salts with corresponding azides **49a-c**. Treatment of mesylate **48b** with thiocarboxylic acid in DMF produced diastereomixtures of thioesters **52a,b** and 3-cyclohexene **50**. Thus, compounds **52a,b** were also separated by MPLC, and regioisomer **52c** was obtained as a diastereomixture (*cis:trans* = 2:1). The synthesized thioesters **52a-c** were reduced with potassium carbonate to give thiols **53a-c**.



Scheme 3. Synthesis of Alkylated Cyclohexane Derivatives. Reagents and conditions: (i) MsCl, Et₃N, DCM, rt; (ii) NaN₃, DMF, 80 °C; (iii) DMP, NaHCO₃, DCM, 0 °C; (iv) Ohira-Bestmann reagent, K₂CO₃, MeOH, 0 °C-rt; (v) CuI, Cy₂NH; (CH₂O)_n, dioxane, reflux.

As shown in Scheme 3, compounds **54-58** were synthesized from alcohol **41**. The azide **55** was obtained by the procedures described above for the synthesis of azide **49**. The aldehyde **56** was obtained by oxidation of alcohol **41** with Dess-Martin periodinate. "Seyferth-Gilbert homologation" of aldehyde **56** was performed using the Ohira-Bestmann reagent and provided a geometrical mixture of alkynes **57**, which were separated into isomers **57a** and **57b** by MPLC. Conversion of alkynes **57a,b** to allenes **58a,b** was achieved by applying the Crabbe Allene synthesis.⁴¹



Scheme 4. Syntheses of α -Naphthoflavone Derivatives. Reagents and conditions: (i) conc. HCl, NaNO₂, NaN₃, THF/H₂O, 0 °C-rt; (ii) 47% HBr in H₂O, AcOH, reflux; (iii) dimethyl thiocarbamoyl chloride, NaH, DMF, 0-80 °C; (iv) 210 °C; (v) 10% NaOH in MeOH, rt.

For comparison with the sp^3 -B-ring, we synthesized ANF derivatives **59-63** (Scheme 4). The azides **59a,b** were obtained by treatment of amines **46a,b** with hydrochloric acid, nitrous acid and sodium azide. Freunderberg-Schonberg thiophenol synthesis was applied to convert the phenol to a thiophenol as follows. The methoxy groups of **47a,b** were deprotected using hydrogen bromide to afford phenols **60a,b**, which were then treated with thiocarbonyl chloride to give thiocarbamates **61a,b**. Thermal rearrangement of thiocarbamates **61a,b** at 210 °C provided carbamothioates **62a,b**, which was followed by hydrolysis with 10% sodium hydroxide in methanol to give thiophenols **63a,b**.

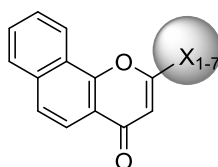
2.3. Inhibitory Activities of Synthetic Compounds toward CYP1B1, CYP1A1 and CYP1A2

The inhibitory potency of the synthetic compounds was determined using the EROD assay,⁴² which measures fluorescence intensity as the enzymatic activity. Screening of the inhibitory activity was evaluated as the relative fluorescence intensity at 1 μ M compound (defined as % activity), when the fluorescence intensity at 0.5% DMSO in the reaction solution was taken as 100%.

To verify suitable sp^3 -B-ring structures for selective CYP1B1 inhibition, we first performed the screening on synthetic benzo[*h*]chromone derivatives with simple sp^3 -B-ring moieties, compounds **37** and **42-45** (Table 1). ANF as a reference aromatic compound completely inhibited CYP1B1, CYP1A1 and CYP1A2 activities at 1 μ M. Some compounds including ANF showed % activity of minus, it might be that not only inhibition of CYP1B1 EROD-activity but also background enzyme in microsomes as reported by Dutour et al.⁴³ The bulky sp^3 -B-ring groups in norbornene endo-**44**, exo-

44 and adamantane **45** showed poor inhibitory potency against CYP1B1 (% activity of 74-89%), reflecting the planar cavity of the CYP1 family. Cyclohexane **37** was more potent than cyclopentane **42**, and was a selective inhibitor of CYP1B1 at 25, 52 and 52% for CYP1B1, CYP1A1 and CYP1A2, respectively, in spite of its large B-ring structure. These findings indicated that the planar cavity in CYP1B1 adapted to accommodate the cyclohexane B-ring having 3D property, as we expected. Although 1-cyclohexene **43** showed strong CYP1B1 inhibitory potency comparable to ANF, the CYP1A1 activity was also completely inhibited at 1 μ M of **43**. On the other hand, 3-cyclohexene **50** did not completely inhibit CYP1B1 activity (% activity of $6.5 \pm 6.7\%$). It is considered that the double bond position in the cyclohexene ring near the benzo[*h*]chromone skeleton contributes to the molecular planarity. Because the cyclohexyl-containing derivative has sufficient inhibitory potency, we selected compound **37** as a lead compound reflecting the 3D characteristic and optimized the activity by adding substituents on the cyclohexane B-ring.

Table 1. Inhibition of CYP1 family activity by benzo[*h*]chromone derivatives containing various B-ring structures.



compd	X	X name	%Activity at 1 μ M compound ^a		
			CYP1B1	CYP1A1	CYP1A2
37	X ₁	cyclohexyl	25.4 \pm 1.8	51.5 \pm 2.4	51.8 \pm 2.8

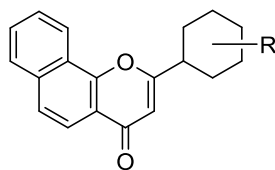
42	X ₂	cyclopentyl	55.3 ± 6.3	28.0 ± 1.9	34.5 ± 3.9
43	X ₃	1-cyclohexenyl	-12.9 ± 5.0	3.2 ± 0.6	21.2 ± 5.4
exo-44	X ₄	5-norbornyl	83.0 ± 7.0	61.0 ± 1.7	34.0 ± 6.3
endo-44	X ₄	5-norbornyl	74.0 ± 8.1	43.0 ± 5.0	0.0 ± 5.7
45	X ₅	adamantyl	89.0 ± 2.8	53.9 ± 4.6	77.8 ± 8.1
ANF	X ₆	phenyl	-11.3 ± 2.7	0.4 ± 0.7	-10.1 ± 1.9
50	X ₇	3-cyclohexenyl	6.5 ± 6.7	38.1 ± 3.3	36.9 ± 4.7

^aEROD-activity by hCYP1 family in the presence of NADPH. The enzymatic activity at 0.5% DMSO in the reaction solution was taken as 100%. The experiment performed in triplicate (\pm SE).

Screening results of the cyclohexane B-ring derivatives (Table 2) demonstrated that introduction of alcohol (**40a-d**, **41**), mesylate (**48a-d**) and amine (**51a-c**) groups regardless of regio- and geometrical isomerism reduced the inhibitory potency against the CYP1 family, which implied that the cyclohexane B-ring was surrounded by hydrophobic residues in the substrate-binding cavity.

Methylated **38** and isopropylated **39** had similar inhibitory potency to compound **37**. It is suggested that the C(4') position was capable of a certain size of hydrophobic substituent. Notably, azide (**49a-c**, **55**), thioacetyl (**52a-c**) and thiol (**53a-c**) derivatives showed more potent inhibitory activity. In particular, azide-containing derivatives **49a-c** and **55** showed better CYP1B1 inhibitory activity and selectivity. To conduct a fine structure activity relationship study, we evaluated compounds **58a,b** containing an allene structure instead of the azide group. Compounds **58a,b** were also strong inhibitors against CYP1B1, which suggested that rigid and linear structures improved the hCYP1B1 inhibition.

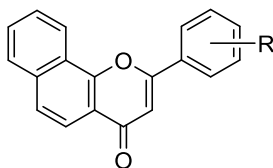
Table 2. Screening of inhibitory potency against CYP1 family by cyclohexane B-ring derivatives.



compd	R	isomer	% Activity at 1 μ M compound ^a		
			CYP1B1	CYP1A1	CYP1A2
38	4'-CH ₃	<i>cis:trans</i> = 3:1	23.9 \pm 1.1	50.2 \pm 4.1	63.0 \pm 7.1
39	4'-iPr	<i>cis:trans</i> = 4:1	27.9 \pm 1.4	48.3 \pm 1.2	N/A ^b
40a	4'-OH	<i>cis</i>	90.4 \pm 1.8	87.3 \pm 3.4	77.3 \pm 4.9
40b	4'-OH	<i>trans</i>	51.3 \pm 1.1	72.7 \pm 0.9	76.2 \pm 2.2
40c	3'-OH	<i>cis</i>	79.4 \pm 1.6	71.3 \pm 0.7	68.2 \pm 3.5
40d	3'-OH	<i>trans</i>	72.9 \pm 1.1	78.0 \pm 2.0	73.9 \pm 6.5
41	4'-CH ₂ OH	<i>cis:trans</i> = 1:1	56.9 \pm 0.4	85.9 \pm 1.2	92.7 \pm 13.4
48a	4'-OMs	<i>cis</i>	51.5 \pm 0.8	66.1 \pm 1.0	57.7 \pm 2.4
48b	4'-OMs	<i>trans</i>	72.5 \pm 2.8	69.9 \pm 0.6	80.3 \pm 3.7
48c	3'-OMs	<i>cis</i>	80.5 \pm 1.0	38.6 \pm 0.9	79.1 \pm 4.9
48d	3'-OMs	<i>trans</i>	59.9 \pm 1.5	66.5 \pm 2.1	69.1 \pm 1.7
54	4'-CH ₂ OMs	<i>cis:trans</i> = 1:1	50.1 \pm 0.8	78.1 \pm 1.7	96.4 \pm 8.0
49a	4'-N ₃	<i>cis</i>	-15.3 \pm 1.6	39.6 \pm 0.2	29.6 \pm 7.1
49b	4'-N ₃	<i>trans</i>	-1.8 \pm 4.1	39.5 \pm 2.9	46.5 \pm 8.3
49c	3'-N ₃	<i>cis:trans</i> = 1:1	-4.0 \pm 4.3	36.1 \pm 2.0	42.5 \pm 3.5
55	4'-CH ₂ N ₃	<i>cis:trans</i> = 2:3	2.2 \pm 0.5	6.3 \pm 2.1	22.3 \pm 3.2
51a	4'-NH ₂	<i>cis</i>	81.6 \pm 2.0	73.7 \pm 2.0	74.5 \pm 4.8
51b	4'-NH ₂	<i>trans</i>	89.5 \pm 0.7	84.2 \pm 2.2	95.4 \pm 4.5
51c	3'-NH ₂	<i>cis:trans</i> = 1:1	64.7 \pm 1.2	80.9 \pm 2.6	44.5 \pm 1.0
52a	4'-SAc	<i>cis</i>	-1.3 \pm 4.0	3.8 \pm 1.1	42.7 \pm 2.8
52b	4'-SAc	<i>trans</i>	-4.7 \pm 5.5	1.1 \pm 0.7	45.4 \pm 3.1
52c	3'-SAc	<i>cis:trans</i> = 2:1	4.4 \pm 0.9	31.7 \pm 1.4	0.5 \pm 1.4
53a	4'-SH	<i>cis</i>	0.5 \pm 0.7	3.9 \pm 0.3	N/A ^b
53b	4'-SH	<i>trans</i>	1.8 \pm 0.2	1.3 \pm 1.3	0.6 \pm 4.0
53c	3'-SH	<i>cis:trans</i> = 3:1	-2.5 \pm 0.3	0.0 \pm 0.4	N/A ^b
57a	4'-CCH	<i>cis</i>	0.9 \pm 0.4	11.3 \pm 1.6	21.0 \pm 4.0
57b	4'-CCH	<i>trans</i>	15.0 \pm 1.1	0.5 \pm 0.8	8.8 \pm 2.2

58a	4'-Allene	<i>cis</i>	3.1 ± 1.0	5.5 ± 1.0	4.3 ± 8.2
58b	4'-Allene	<i>trans</i>	-0.4 ± 0.6	3.0 ± 0.9	-4.5 ± 6.8

^aEROD-activity by hCYP1 family in the presence of NADPH. The enzymatic activity at 0.5% DMSO in the reaction solution was taken as 100%. The experiment performed in triplicate (\pm SE). ^bNot analyzed

Table 3. Screening of inhibitory potency against CYP1 family by ANF derivatives.

compd	R	%Activity at 1 μ M compound ^a		
		CYP1B1	CYP1A1	CYP1A2
46a	4'-NH ₂	-1.2 \pm 0.8	2.1 \pm 1.7	-16.3 \pm 2.1
46b	3'-NH ₂	0.2 \pm 0.6	7.6 \pm 1.0	-3.5 \pm 5.8
47a	4'-OMe	-0.5 \pm 0.3	4.0 \pm 2.4	15.9 \pm 12.0
47b	3'-OMe	1.9 \pm 0.6	8.7 \pm 0.2	6.1 \pm 5.3
59a	4'-N ₃	-0.5 \pm 0.9	2.3 \pm 2.2	-13.6 \pm 5.0
59b	3'-N ₃	0.7 \pm 0.8	1.4 \pm 1.1	6.9 \pm 8.4
60a	4'-OH	3.7 \pm 0.2	6.3 \pm 1.1	10.4 \pm 6.9
60b	3'-OH	1.6 \pm 0.9	8.2 \pm 0.5	37.2 \pm 6.4
61a	4'-OC(=S)NMe ₂	15.1 \pm 1.2	17.6 \pm 0.4	96.9 \pm 7.4
61b	3'-OC(=S)NMe ₂	2.5 \pm 1.0	3.1 \pm 1.2	75.4 \pm 2.1
62a	4'-SC(=O)NMe ₂	12.3 \pm 0.3	10.3 \pm 1.7	91.9 \pm 5.3
62b	3'-SC(=O)NMe ₂	2.4 \pm 0.6	3.8 \pm 0.7	68.7 \pm 8.8
63a	4'-SH	54.3 \pm 0.4	71.3 \pm 3.2	106.4 \pm 9.6
63b	3'-SH	9.8 \pm 1.4	18.7 \pm 0.5	56.2 \pm 1.7

^aEROD-activity by hCYP1 family in the presence of NADPH. The enzymatic activity at 0.5% DMSO in the reaction solution was taken as 100%. The experiment performed in triplicate (\pm SE).

The simple transformation from aromatic to non-aromatic B-rings (Table 3) gives rise to a notable difference in the CYP1 inhibitory properties. Most synthetic ANF derivatives, even those containing alcohol (**60a,b**) or amine (**46a,b**) groups, strongly inhibited the enzymatic activities of CYP1B1, CYP1A1 and CYP1A2 at 1 μ M, \leq 10%, except for **60b** of CYP1A2. Introduction of a thiol group

increased the inhibitory activity among the cyclohexane B-ring derivatives, but in the case of an aromatic B-ring, it reduced the CYP1B1 inhibitory activity, e.g., **63a** (54%) and **63b** (9.8 %). These differences demonstrated that the 3D-structural property is an important factor for the selectivity and inhibitory activity among the CYP1 family.

From these results, we found strong CYP1B1 inhibitors having sp^3 -B-rings that included azide, allene, thiol and thioacetyl groups. To investigate their inhibitory potency against the CYP1 family in more detail, we determined the IC_{50} values of the compounds (Table 4).

The compound **49a** showed stronger inhibitory potency (IC_{50} of 4.4 nM for CYP1B1) than that of ANF (IC_{50} of 10.6 nM). Moreover, among the evaluated compounds, **49a** showed the highest selective inhibition against CYP1B1 at 120-times over CYP1A1 and CYP1A2 (IC_{50} of 525 and 667 nM for CYP1A1 and CYP1A2, respectively). *trans*-Isomer **49b** had 100-times lower inhibitory activity against CYP1B1 (IC_{50} of 134 nM) than *cis*-isomer **49a**. Interestingly, all azide derivatives (**49a-c**, **55**) showed selectivity for hCYP1B1. Although they had a linear structure, allene derivatives showed a different inhibitory activity profile than the azide derivatives. Stronger CYP1B1 inhibition was found for the *trans*-isomer **58b** (IC_{50} of 13.4 nM) than the *cis*-isomer **58a** (IC_{50} of 68.1 nM). Moreover, it did not have selectivity among the CYP1 family. These results revealed that the allene group and the azide group are not equivalent in CYPs inhibition. Concerning other substituents, thioesters **52a,b** exhibited more inhibitory potency against CYP1B1 than thiols **53a-c**, but less than **49a**. Thus, we concluded that

the most effective substituent for the cyclohexane B-ring derivative is the azide group. In the case of aromatic B-rings, compounds **59a,b** having an azide substituent at C(4') or C(3') showed strong inhibitory potency against not only CYP1B1 but also CYP1A1. Therefore, these compounds had low selectivity compared to the series of cyclohexane B-rings. In this way, our strategy using sp³ carbons in the B-ring allowed us to discover the selective CYP1B1 inhibitor **49a**.

Table 4. Inhibition of CYP1B1, CYP1A1, CYP1A2 activity and selectivity by hit compounds.

compd	R	isomer	IC ₅₀ (nM)			IC ₅₀ ratio ^a	
			CYP1B1	CYP1A1	CYP1A2	1A1/1B1	1A2/1B1
<i>Cyclohexyl B-ring</i>							
49a	4'-N ₃	<i>cis</i>	4.4	525	667	120.4	153
49b	4'-N ₃	<i>trans</i>	134.6	1036	1190	7.7	8.8
49c	3'-N ₃	<i>cis:trans</i> = 1:1	90.3	N/A ^b	N/A ^b		
55	4'-CH ₂ N ₃	<i>cis:trans</i> = 2:3	23.5	215.6	432.8	9.2	18.5
58a	4'-Allene	<i>cis</i>	68.1	33.	N/Ab	0.48	
58b	4'-Allene	<i>trans</i>	13.4	13.6	36.4	1.02	2.7
52a	4'-SAc	<i>cis</i>	24.3	65.	N/A ^b	2.7	
52b	4'-SAc	<i>trans</i>	29.4	15.9	991	0.54	33.7
53a	4'-SH	<i>cis</i>	38.8	76.2	N/A ^b	1.97	
53b	4'-SH	<i>trans</i>	40.3	146	689	3.6	17.1
53c	3'-SH	<i>cis:trans</i> = 3:1	66.1	133.5	N/A ^b	2.02	
37	H	none	539.8	N/A ^b	N/A ^b		
<i>Phenyl B-ring</i>							
59a	4'-N ₃	none	2.6	9.5	93.8	3.6	35.6
59b	3'-N ₃	none	1.8	27.1	74.7	15.5	42.8
60a	4'-OH	none	43.4	43	908.7	0.99	21
ANF	H	none	10.6	53.8	68.4	5.1	6.5

^aIC₅₀ (CYP1A1)/IC₅₀ (CYP1B1) or IC₅₀ (CYP1A2)/IC₅₀ (CYP1B1). ^bNot analyzed.

2.4. Comparing Solubilities of ANF, **37**, **49a** and **59a**

In order to examine the influence of dearomatization and addition of azide group on solubility, the thermodynamic aqueous solubility of ANF and compounds **37**, **49a**, **59a** was evaluated with the saturation shake-flask method.⁴⁴ ANF is known to have quite low solubility in aqueous solvent due to its planar and hydrophobic structure. We also observed that ANF was nearly insoluble in PBS (pH 7.4), and therefore used a solution in which PBS and ethanol were mixed at 9:1 as the solvent for solubility measurements. However, the solubility of ANF was still poor (2.63 μM) in this solution. Aromatic B-ring-linked azide **59a** showed the worst solubility (<1 μM) in this series. On the other hand, dearomatization of the B-ring improved the aqueous solubility. Indeed, cyclohexane B-ring **37** was 3.7-times more soluble (9.65 μM) than ANF. Cyclohexane B-ring-linked azide **49a** retained this solubility (2.67 μM) compared with ANF. Lipophilicity was also important for water solubility. Introduction of the azide (from ANF to **59a**, from **37** to **49a**) increased the CLogP (>0.17) with decreasing solubility, which could be caused by its hydrophobicity. In contrast, dearomatization of the B-ring (from ANF to **37**, from **59a** to **49a**) also increased ClogP (>0.5) but improved solubility. Thus, we demonstrated that the increasing complexity induced by the sp^3 -B-ring contributes to the aqueous solubility.

2.5. Spectroscopic Analysis

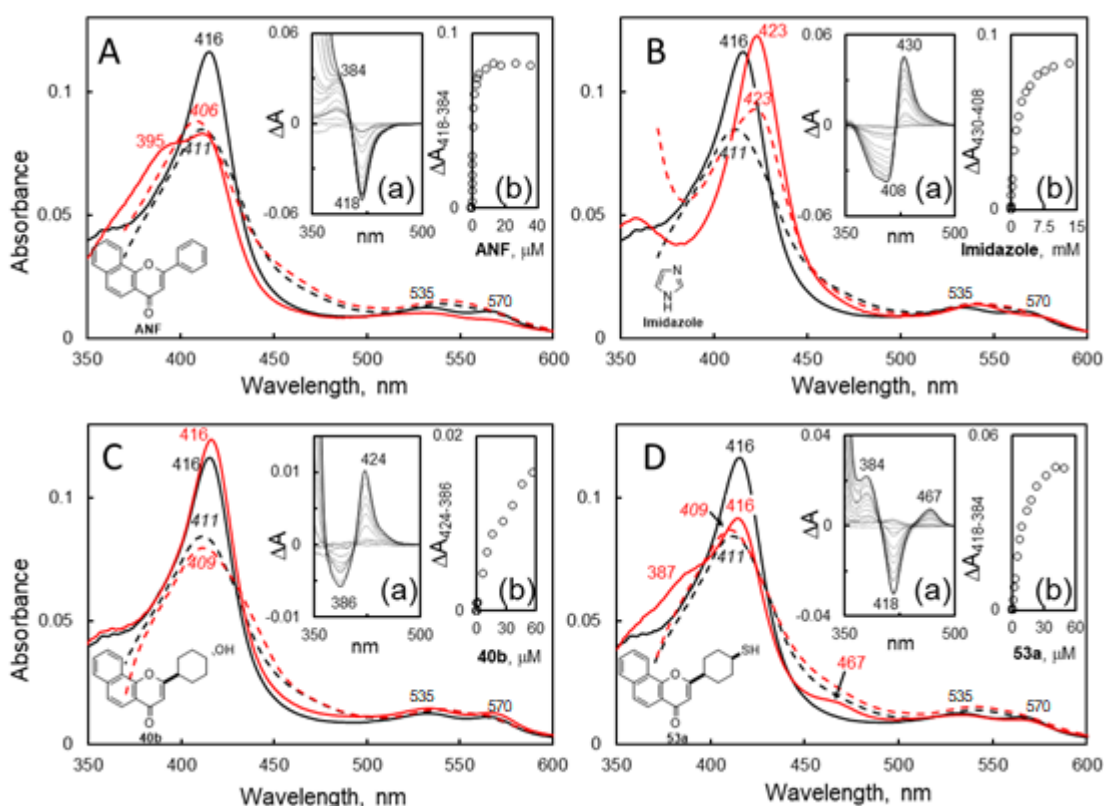


Figure 4. Spectral changes induced in hCYP1B1 upon binding of ANF (A), imidazole (B), 40b (C), and 53a (D). Shown are absorbance spectra of Fe^{3+} state (black line), Fe^{3+} state w/ inhibitor (red line), Fe^{2+} state (black dashed line) and Fe^{2+} w/ inhibitor (red dashed line). Concentrations of hCYP1B1, ANF, imidazole, 40b and 53a are 1 μM , 5 μM , 10 mM, 120 μM , and 50 μM . Insets (a) are difference spectral changes observed during titration of hCYP1B1 with different ligands. Insets (b) show plots of spectral change vs. ligand concentration. The types of spectral change were type 1 (Fe^{3+} -5th state, A), type 2 (N- Fe^{3+} -6th state, B), reverse type 1 (O- Fe^{3+} -6th state, C) and S- Fe^{3+} -6th state (D). Oxidative state of iron changed from ferric to ferrous by addition of $\text{Na}_2\text{S}_2\text{O}_4$.

In order to determine the manner of interaction, we measured the ultraviolet-visible (UV-vis) absorbance changes of CYP1B1 introduced by the inhibitor. The absorbance spectrum of CYP is characterized by the spin and oxidized states of heme⁴⁵ and thus reflects the binding of a “ligand”. CYP1B1 was expressed in *Escherichia coli* (E. Coli) and purified in the absence of ANF by applying

previously reported methods.²⁸ The steady state absorption spectra showed peaks at 416, 535 and 570 nm in the Soret, β - and α regions,⁴⁶ which are representative of low spin state spectra along with water coordination⁴⁶ (Figure 4).

Addition of ANF induced a type 1 spectral change⁴⁶ (Fig. 4A). The spectral characteristics suggested that ANF excluded the sixth water ligand of the heme and thus interacted with CYP1B1 without a water ligand in the co-crystal structure.³² In the same way, cyclohexyl azides **49a,b**, **55**, phenyl azides **59a**, **59b**, and compounds **37-39**, **43**, **50**, **52a**, **53b**, **57a** and **58a,b** also showed type 1 spectral changes (Table 5). Moreover, we observed not only type 1 spectral changes but three other types of representative spectral changes: (1) imidazole and amine compounds **51a**, **51c** induced type 2 spectral changes⁴⁷ (Fig. 4B) that reflect the coordination of a nitrogen atom; (2) alcohols **40a-b** and compounds **51b**, **52b**, **57b** showed reverse (rev.) type 1 spectral changes⁴⁸ (Fig. 4C) indicating coordination of oxygen atoms; (3) thiol groups **53a,c** induced a distinctive spectral change (Fig. 4D) reflecting coordination of thiol groups.⁴⁹ In regards to the oxidation state, the reduced CYP1B1 spectrum showed the same features as other CYPs.^{46,50} In this way, our synthetic inhibitors induced distinctive spectral changes corresponding to the substituent structure at the B-ring. We confirmed by spectroscopic analysis that the cyclohexane B-ring was located toward the heme, similar to ANF, despite the nonaromatic B-ring.

Table 5. Spectral Interaction of Synthetic Inhibitors with hCYP1B1^a.

compd	R	isomer	wavelength (peak/trough)	Ks ^b (μ M)	ΔA ($A_{\max} - A_{\min}$)	$\Delta A/Ks$	type
<i>Cyclohexenyl B-ring</i>							
43	H	1-cyclohexenyl	384/418	1.1	0.098	0.0892	1
50	H	3-cyclohexenyl	384/418	3.1	0.033	0.0104	1
<i>Cyclohexanyl B-ring</i>							
37	H		384/416	5.9	0.019	0.0033	1
38	4'-Me	3:1	385/418	5.7	0.035	0.0062	1
39	4'-iPr	4:1	384/416	124.1	0.046	0.0004	1
40a	4'-OH	<i>cis</i>	420/385	>1218	>0.1945	0.0005	rev. 1
40b	4'-OH	<i>trans</i>	424/386	62.7	0.032	N.D. ^d	rev. 1
49a	4'-N ₃	<i>cis</i>	384/418	2.6	0.075	0.0284	1
49b	4'-N ₃	<i>trans</i>	384/418	5.4	0.053	0.0098	1
55	4'-CH ₂ N ₃	2:3	384/418	3.9	0.059	0.0152	1
51a	4'-NH ₂	<i>cis</i>	428/N.D. ^d	N.D. ^d	N.D. ^d	N.D. ^d	2
51b	4'-NH ₂	<i>trans</i>	417/389	N.D. ^d	N.D. ^d	N.D. ^d	rev. 1
51c	3'-NH ₂	1:1	442/418	2.9	0.012	0.0040	2
52a	4'-SAc	<i>cis</i>	384/418	4.0	0.084	0.0208	1
52b	4'-SAc	<i>trans</i>	424/384	6.7	0.035	0.0052	rev. 1
53a	4'-SH	<i>cis</i>	384/418	9.4	0.055	0.0059	1 ^c
53b	4'-SH	<i>trans</i>	384/417	8.9	0.053	0.0060	1
53c	3'-SH	3:1	384/418	8.1	0.044	0.0054	1 ^c
57a	4'-CCH	<i>cis</i>	384/416	7.3	0.024	0.0033	1
57b	4'-CCH	<i>trans</i>	424/387	263.9	0.033	0.0001	rev. 1
58a	4'-Allene	<i>cis</i>	384/417	25.4	0.023	0.0009	1
58b	4'-Allene	<i>trans</i>	384/415	2.4	0.019	0.0081	1
<i>Phenyl B-ring</i>							
59a	4'-N ₃		384/418	0.9	0.082	0.0879	1
59b	3'-N ₃		384/418	0.8	0.070	0.0922	1
ANF	H		384/418	0.7	0.083	0.1281	1
<i>Other Structure</i>							
Imidazole			430/408	1255.0	0.092	0.0001	2

^aDetection by difference spectrum in the presence of inhibitor. ^bSpectral dissociation constant. ^cS-coordination. ^dNot detected.

The binding affinity of the synthetic inhibitors was evaluated as the spectral dissociation constant (K_s) and magnitude of spectral binding ($\Delta A/K_s$) calculated from equilibrium titrations (Table 5). Comparing the six-membered B-ring structures, the binding affinity was higher in the order of ANF, 1-cyclohexenyl **43**, 3-cyclohexenyl **50** and cyclohexyl **37** (K_s : 0.7, 1.1, 3.1 and 5.9 μM , respectively), with the same order of CYP1B1 inhibition. Spectroscopic analysis supported that the molecular planarity has a critical influence on binding to CYP1B1.

Cyclohexyl azides **49a,b**, **55** and phenyl azides **59a,b** induced spectral shape changes ($\Delta A > 0.05$) and thus had high binding affinity for CYP1B1 (K_s : 0.8-5.4 μM). The order of binding affinity was the same as the order of inhibitory activity. Interestingly, the phenyl azide itself did not show binding affinity or inhibition activity at all (data not shown). In comparison with the *cis*-**49a** and *trans*-**49b** azides ($\Delta A/K_s$ of 0.0284 and 0.0098, respectively), the *cis*-**58a** and *trans*-**58b** allenes showed weaker binding affinity ($\Delta A/K_s$ of 0.0009 and 0.0081, respectively) derived from their small absorption changes (ΔA of ~ 0.02). Spectroscopic analysis also showed the difference between azide and allene.

2.6. X-ray Crystal Structure Analysis

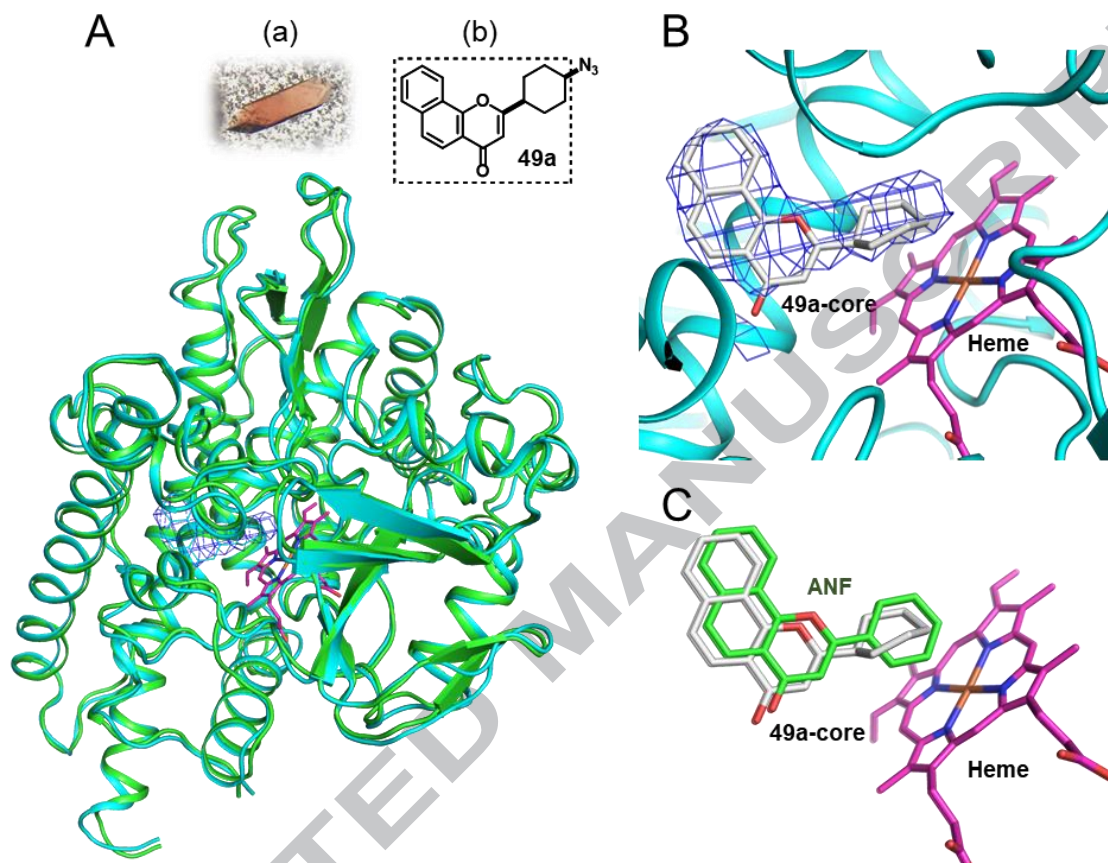


Figure 5. Overall structure of compound 49a/CYP1B1 (A), and substrate binding site (B and C). A shows superposition of **49a**/CYP1B1 (*cyan*) and ANF/CYP1B1 (*green*). The $2F_o - F_c$ map (*blue mesh*) positioned substrate binding site. The A-D ring of **49a** (*49a-core*) conformed the electron density map, but the localization of azide can not be confirmed (B). C shows conformational comparison of *49a-core* and ANF (*green stick*)/CYP1B1. (a) shows co-crystal of **49a**/CYP1B1. (b) shows **49a** structure and *49a-core* (*dash line*).

We co-crystallized compound **49a** and hCYP1B1 to investigate the binding mode by X-ray crystal structure analysis. Compound **49a** was added after purification of CYP1B1. The complex of compound **49a** and CYP1B1 was crystallized by the hanging drop vapor diffusion method. In this way,

we successfully obtained a deep red crystal for the X-ray diffraction experiment and X-ray crystal structure analysis (Figure 5). The data collection and refinement statistics are summarized in Table S1.

The overall structure of CYP1B1/**49a** (6IQ5. pdb) exhibits a canonical P450-fold and overlaps with the structure of hCYP1B1/ANF (Fig. 5A). The electron density map of compound **49a** exists in the substrate-binding site around the heme, the same location that ANF occupies (Fig. 5B and 5C). In spite of the transformation of the B-ring structure from phenyl to cyclohexyl, we confirmed the localization of the CD-ring, which was in a position corresponding to ANF. The conformation of the cyclohexyl B-ring, clearly different from that of ANF, was twisted against the planar surface of the CD-ring. While we could confirm the location of the skeleton of compound **49a** by X-ray crystal structure analysis, it was difficult to determine of positioning of terminal nitrogen atom due to low resolution.

2.7. Docking Analysis

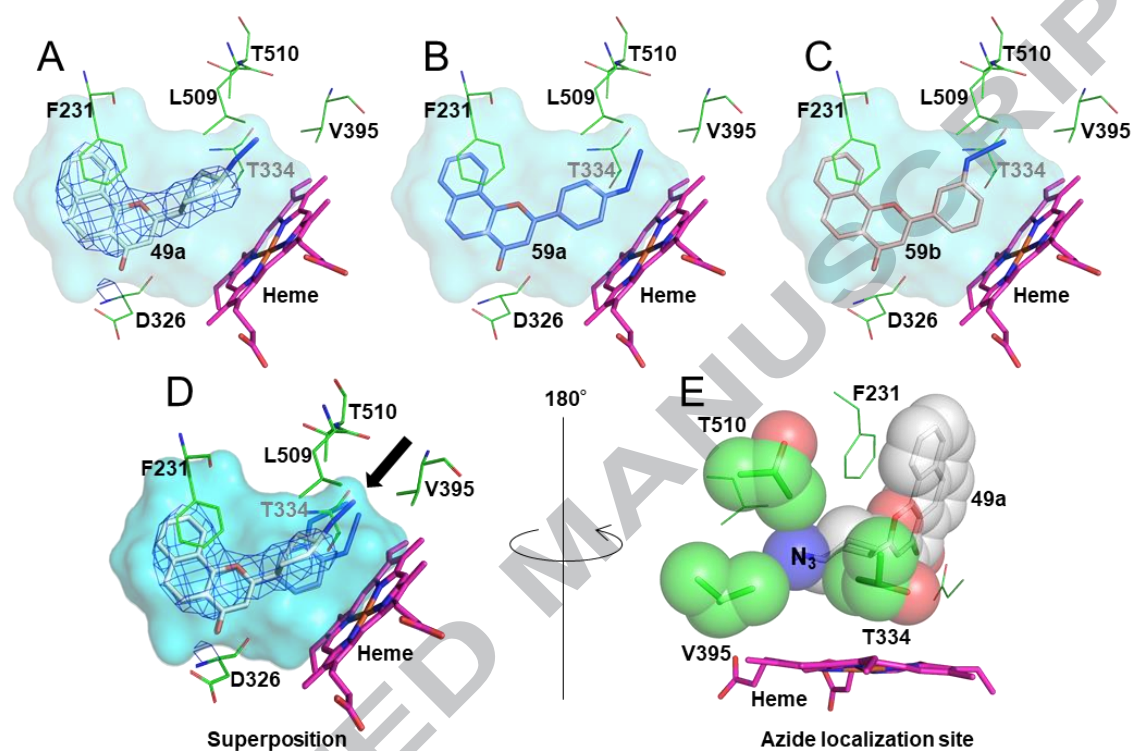


Figure 6. The localization site of azide substitute in CYP1B1. Docking model of **49a** (A), **59a** (B) and **59b** (C) are shown as stick model in *white*, *blue* and *salmon*, respectively. The electron density map (*blue mesh*) observed by X-ray crystal structure analysis is displayed. Residues of CYP1B1 are shown in *green*. *D* shows superposition of docking model (A-C) and the localization site of azide indicated by *black arrow*. *E* is a view of *D* from the opposite side, which shows **49a** and the localization site of azide as translucent sphere model.

To elucidate the location of the azide substituent in compound **49a**, we performed docking analysis using the Surflex Dock program on Sybyl X2 (Tripos) software. We obtained two types of docking models: (1) the B-ring is in a twisted conformation that is well fit to the electron density map of the X-ray crystal structure of **49a** (Fig. 6A), (2) a conformation similar to that of ANF in hCYP1B1 for

59a and **59b** (Fig. 6B and 6C). All compounds were surrounded by hydrophobic amino acid residues in similar with observed crystal structure. The CD-ring in both types of conformation formed a π - π interaction with Phe231 and the B-ring had intimate interaction with Leu509. Three docking models suggested that localization of the terminal nitrogen atom of the azide converged in a tiny hydrophobic cavity constructed by Thr334, Val395 and Thr510 (Fig. 6C and 6D). Thus, we demonstrated that hydrophobic interactions play an important role for the binding affinity and inhibitory potency of compound **49a**. However, CYP1A1 also conserved the residues of Thr321, Val382 and Thr497 as in CYP1B1.

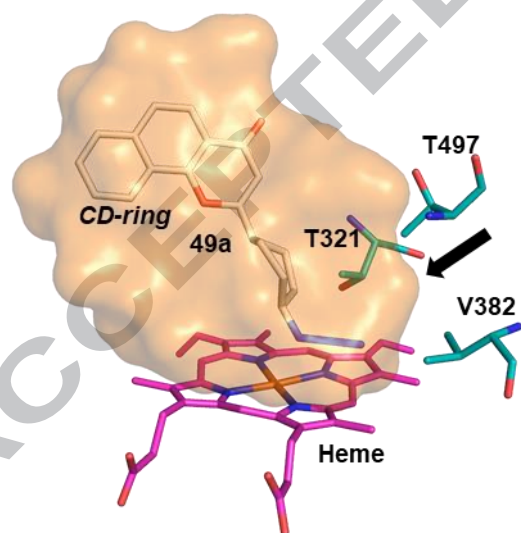


Figure 7. Docking model of compound 49a in CYP1A1. Docking model of **49a** (*white*), the heme (*magenta*) and residues (*teal*) are shown as stick models in atom type. Cavity of CYP1A1 is illustrated in *orange*. *Black arrow* shows the localization site of azide in CYP1B1. Azide substitute of **49a** does not interact with the site in this model.

We constructed the docking model of compound **49a** and CYP1A1 to discuss the selectivity (Figure 7). In this analysis, because the benzo[*h*]chromone core was observed in a similar conformation as was ANF in CYP1B1, we restricted the conformation of the CD-ring to be identical to that of the ANF/CYP1A1 crystal structure. This docking simulation supports the reason why azide **49a** lacks CYP1A1 affinity. There is an absence of interaction between the azide substituent and the cavity as judged by the distance between them. Thus, we concluded that the conformation of the benzo[*h*]chromone core in CYP1A1 and CYP1A2 was unsuitable for compound **49a**. In addition, instead of Val395 as in CYP1B1, CYP1A2 has a Leu382 which is a bulkier residue, therefore it is more difficult to accept the azide group.

The residue at position 395 in CYP1B1 has been reported to be critical factor for catalytic activity and substrate recognition.^{51,52} We considered that the difference in binding affinity between *cis*-azide **49a** and *cis*-allene **59a** was caused by acceptability of this tiny site. As a reason for this, the terminal carbon atom of the allene has two perpendicular hydrogen atoms. Although these reasons are not valid for all our synthetic compounds, we deduced that the complexity caused by the combination of the cyclohexane structure, the azide substituent and the benzo[*h*]chromone core effectively enforces the desired selectivity for hCYP1B1 among the highly homologous CYP1 family.

3. Conclusion

We designed and synthesized a series of benzo[*h*]chromone derivatives with linked nonaromatic B-rings to improve the selectivity for CYP1B1 and the solubility of ANF as a lead compound. EROD assays demonstrated that cyclohexane-linked benzo[*h*]chromone **37** was suitable for hCYP1B1 inhibition by comparison of B-ring structures composed of sp³ carbons. Screening of substituents on compound **37** revealed that the azide-containing *cis*-**49a** exhibited 120-times higher selectivity for CYP1B1 than CYP1A1 and CYP1A2 and possessed stronger inhibitory potency than ANF. On the other hand, the azide-containing naphthoflavone **59a** showed strong inhibitory potency but low selectivity. For this reason, we confirmed that the azide substituent increased the inhibitory potency and the cyclohexane structure was effective for CYP1B1 selectivity. Moreover, we found that compound **37** was more soluble in aqueous solution than ANF, and therefore demonstrated that the conversion of the benzene B-ring to the cyclohexane B-ring improved the solubility. The solubility of compound **49a** decreased upon introduction of the azide substituent, but was still equal to or greater than that of ANF. In this way, we synthesized a selective and strong CYP1B1 inhibitor without decreasing the water solubility.

We then investigated the manner of binding between the synthetic inhibitor and CYP1B1. Spectroscopic analysis showed that the synthetic inhibitors induced distinctive spectral changes in CYP1B1 corresponding to the substituent structure at the B-ring, and thus suggested that the

cyclohexane B-ring was located near the heme. Moreover, compounds **49a**, **59a** and **59b**, which have strong inhibitory potency, showed high binding affinity for CYP1B1. Therefore, this method could provide important information to determine the binding manner and potency of CYP1B1 inhibitors. X-ray crystal structure analysis revealed that the conformation of the benzo[*h*]chromone core in compound **49a** was similar to the conformation of ANF in hCYP1B1, but the azide substituent could not be located due to low resolution. Three docking models of hCYP1B1 indicated that the azide substituent was located in the small and hydrophobic site formed by Thr334, Val395 and Thr510. Therefore, the selectivity could be controlled by the difference in acceptability of the site among CYP1B1, CYP1A1 and CYP1A2. The increasing complexity caused by sp^3 carbons was also accommodated in the planar cavity. These results promise to be useful for the design of novel CYP1B1 inhibitors.

4. Experimental procedures

4.1. General Experimental Procedures.

All reagents were purchased from commercial sources and were used without further purification. Organic solvents were dried by standard methods. All air and moisture sensitive reactions were carried out under nitrogen atmosphere. Unless otherwise stated, NMR spectra were recorded at 300, 400 MHz for ^1H NMR and 75, 100 MHz for ^{13}C NMR in CDCl_3 solution with TMS as an internal standard and the chemical shifts are given in δ values. High resolution mass spectra were obtained using JEOL AccuTOF LC-plus JMS-T100LP spectrometer. Purity was determined by HPLC [Pegasil silica SP100, 4.6 mm \times 150 mm, CHCl_3 or hexane/ CHCl_3 (3:7) or hexane/ CHCl_3 (7:3), flow rate 1.0 mL/min] and was >95% for compounds which was used to EROD-assay tested.

4.2 Synthesis

4.2.1. General Procedures for (tert-Butyldimethylsilyloxy)cyclohexane carboxylic acid (6a-c, 7).

To a solution of **4a** (1.22 g, 8.45 mmol) and *tert*-butyldimethylsilyl chloride (2.80 g, 18.6 mmol) in dry DMF (17 mL) was added triethylamine (2.6 mL, 18.6 mmol) at room temperature. After being stirred for 2h, the reaction mixture was quenched with ice water, acidified with 1 M hydrochloric acid, and diluted with ether. The organic layer was separated, washed with brine and evaporated. The residue was immediately used in further reaction.

To a solution of the crude product in 50% MeOH/THF (14 mL) was added 5M NaOH (2 mL) at room temperature. After being stirred for 3 h, the reaction mixture was concentrated to one-half volume and diluted with ether. The aqueous layer washed with ether, acidified with 2M hydrochloric acid, and diluted with ether. The organic layer was separated, washed with brine, dried over MgSO_4 and concentrated to afford **6a** (1.74 g, 80%, 2 steps) as a colorless oil.

cis-4-((*tert*-Butyldimethylsilyloxy)cyclohexane-1-carboxylic acid (**6a**). ^1H -NMR (300 MHz, CDCl_3) δ 3.89-3.84 (1H, m, H-C(4')), 2.31 (1H, dt, $J = 10.1, 3.4$, H-C(1')), 1.98-1.87 (2H, m), 1.69 (4H, m), 1.52-1.42 (2H, m), 0.85 (9H, s, *t*Bu-Si), 0.04 (6H, s, $(\text{Me})_2$ -Si).

trans-4-((*tert*-Butyldimethylsilyloxy)cyclohexane-1-carboxylic acid (**6b**). Yield: 83%, 2 steps, as a colorless oil. ^1H -NMR (300 MHz, CDCl_3) δ 3.63-3.53 (1H, m, H-C(4')), 2.35-2.25 (1H, m, H-C(1')), 2.05-1.99 (2H, m), 1.94-1.87 (2H, m), 1.53-1.27 (4H, m), 0.88 (9H, s, *t*Bu-Si), 0.05 (6H, s, $(\text{Me})_2$ -Si)

3-((*tert*-Butyldimethylsilyloxy)cyclohexane-1-carboxylic acid (**6c**). Yield: 78%, 2 steps, (*cis:trans* = 7:3), as a colorless oil. ^1H NMR (300 MHz, CDCl_3) δ 4.10-4.03 (0.3H, m), 3.68-3.55 (0.7H, m), 2.81 (0.3H, dt, $J = 10.7, 3.7$ Hz), 2.46-2.31 (0.7H, m), 1.97-1.20 (8H, m), 0.91, 0.88 (3:7)(9H, s, *t*Bu-Si), 0.10, 0.06 (3:7)(6H, s, $(\text{Me})_2$ -Si).

4-(((*tert*-Butyldimethylsilyloxy)methyl)cyclohexane-1-carboxylic acid (**7**). Yield: 94%, 2 steps, (*cis:trans* = 17:3), as a white solid. ^1H NMR (300 MHz, CDCl_3) δ 3.43, 3.40 (17:3)(2 H, d, $J = 6.6$ Hz,

CH₂-O), 2.63-2.60 (0.85 H, m, H-C(1)), 2.31-2.20 (0.15 H, m, H-C(1)), 2.09-1.96 (2H, m), 1.68 (4H, m), 1.34-1.19 (2H, m), 0.89, 0.88 (17:3)(9H, s, *t*-Bu-Si), 0.03 (6H, s, (Me)₂-Si).

4.2.2. General Procedures for ((*tert*-Butoxycarbonyl)amino)benzoic acid **13a** and **13b**.

To a solution of **12a** (2.0 g, 14.6 mmol) in 67% 1,4-dioxane/water (48 mL) was added triethylamine (4.07 mL, 29.2 mmol) at room temperature and allowed to stir for 5 min. Di-*tert*-butyl decarbonate (6.37 mL, 29.2 mmol) was then added to the solution. After being stirred for 26 h, the reaction mixture was concentrated and acidified with 2 M hydrochloric acid to yield a white precipitate. The slurry was then filtered, washed with water and dried over *in vacuo* to afford **13a** (2.94 g, 86%) as a white solid.

4-((*tert*-Butoxycarbonyl)amino)benzoic acid (13a). Yield: 86%. ¹H NMR (300 MHz, CDCl₃) δ 8.03 (2H, dt, *J* = 8.8, 2.1 Hz), 7.46 (2H, dt, *J* = 8.9, 2.0 Hz), 6.71 (1H, s, H-N), 1.54 (9H, s, *t*Bu-O).

3-((*tert*-Butoxycarbonyl)amino)benzoic acid (13b). Yield: 94%, as a white solid. ¹H NMR (300 MHz, CDCl₃) δ 8.00 (1H, t, *J* = 1.9 Hz), 7.79-7.70 (2H, m), 7.40 (1H, t, *J* = 7.7 Hz), 6.61 (1H, br.s, H-N), 1.54 (9H, s, *t*Bu-O).

4.2.3. General Procedure for Naphthalene esters (method iv: **15-17**, **20-23**, **25a**, **25b**).

To a solution of **3** (*cis* and *trans* mixtures) (342 μL, 1.99 mmol) in thionyl chloride (173 μL, 2.39 mmol) was added a drop of DMF at room temperature. After being stirred at 40 °C for 40 min, the reaction mixture was evaporated with blowing nitrogen at room temperature. The residue was added a solution of 1-hydroxy-2-acetonaphthone (247 mg, 1.33 mmol) in pyridine (660 μL), heated to 60 °C and then stirred for 1 h. After cooling to room temperature, the reaction was quenched with water and diluted with AcOEt. The organic layer was separated, washed with brine, dried over MgSO₄ and evaporated. The residue was purified by chromatography on NH-silica gel (9 g) with 8% AcOEt/hexane to afford **17** (449 mg, quant, dr 4:1) as colorless oil.

2-Acetylnaphthalen-1-yl cyclohexanecarboxylate (15). Yield: quant, as a light yellow powder. ¹H NMR (300 MHz, CDCl₃) δ 7.98-7.94 (1H, m, H-*Ar*), 7.89-7.86 (1H, m, H-*Ar*), 7.83 (2H, d, *J* = 8.6 Hz, H-*Ar*), 7.77 (1H, d, *J* = 8.6 Hz, H-*Ar*), 7.63-7.53 (2H, m, H-C(6, 7)), 2.82 (1H, tt, *J* = 11.4, 3.6 Hz, H-C(1')), 2.64 (3H, s, Me-C=O), 2.36-2.25 (2H, m), 1.98-1.85 (2H, m), 1.82-1.66 (3H, m), 1.52-1.32 (3H, m).

2-Acetylnaphthalen-1-yl 4-methylcyclohexane-1-carboxylate (16). Yield: 47%, dr 4:1, as a colorless oil. ¹H NMR (300 MHz, CDCl₃) δ 8.01-7.95 (4H, m, H-*Ar*), 7.63-7.53 (2H, m), 3.08-2.99 (0.8H, m, H-C(1')), 2.73 (0.2H, tt, *J* = 12.2, 3.6 Hz, H-C(1')), 2.64 (3H, s, Me-C=O), 2.38-2.17 (2H, m), 1.93-1.80 (2H, m), 1.76-1.64 (2.8H, m), 1.53-1.41 (1.8H, m), 1.17-1.07 (0.4H, m), 0.99, 0.96 (4:1)(3H, d, *J* = 6.5 Hz). (major-isomer) ¹³C NMR (75 MHz, CDCl₃) δ 20.69, 25.89 (2 Carbons), 29.78, 30.2, 31.37 (2 Carbons), 41.19, 122.85, 125.03, 125.76, 126.9, 127.31, 127.6, 127.89, 128.43, 136.2,

146.14, 173.98, 198.14. (minor-isomer) ^{13}C NMR (75 MHz, CDCl_3) δ 22.53, 29.05 (2 Carbons), 29.78, 32.04, 34.28 (2 Carbons), 43.46, 122.81, 125.07, 125.82, 126.81, 127.31, 127.48, 127.89, 128.46, 136.2, 146.14, 174.37, 197.98. HRMS (ESI) calcd. for $\text{C}_{20}\text{H}_{22}\text{O}_3\text{Na}$ $[\text{M} + \text{Na}]^+$ 333.14666, found 333.14596.

2-Acetylnaphthalen-1-yl 4-isopropylcyclohexane-1-carboxylate (17). Yield: quant, dr 4:1. ^1H NMR (300 MHz, CDCl_3) δ 8.03-7.93 (1H, m, H-Ar.), 7.90-7.72 (3H, m, H-Ar.), 7.63-7.51 (2H, m, H-Ar.), 3.11 (0.8H, qui, $J = 4.7$ Hz, H-C(1')), 2.73 (0.2H, dt, $J = 12.3, 3.6$ Hz, H-C(1')), 2.63 (3H, s, Me-C=O), 2.45-2.27 (2H, m), 1.96-1.43 (6.8H, m), 1.28-1.08 (1.2H, m), 0.91 (6H, d, $J = 6.5$ Hz, (Me) $_2$ -CH-). (major-isomer) ^{13}C NMR (75 MHz, CDCl_3) δ 20.08 (2 Carbons), 26.57 (2 Carbons), 26.79 (2 Carbons), 29.78, 31.10, 40.85, 42.82, 122.89, 125.01, 125.76, 126.93, 127.27, 127.61, 127.90, 128.41, 136.19, 146.18, 173.90, 198.14. (minor-isomer) ^{13}C NMR (75 MHz, CDCl_3) δ 19.78 (2 Carbons), 28.90 (2 Carbons), 29.23 (2 Carbons), 29.88, 32.79, 43.32, 43.83, 122.82, 125.07, 125.82, 126.83, 127.27, 127.48, 127.90, 128.46, 136.19, 146.18, 174.33, 197.95. HRMS (ESI) calcd. for $\text{C}_{22}\text{H}_{26}\text{O}_3\text{Na}$ $[\text{M} + \text{Na}]^+$ 367.17796, found 361.17942

2-Acetylnaphthalen-1-yl cyclopentanecarboxylate (20). Yield: quant, as a light yellow powder. ^1H NMR (300 MHz, CDCl_3) δ 7.98-7.94 (1H, m), 7.89-7.86 (1H, m, H-Ar), 7.83 (1H, d, $J = 8.6$ Hz, H-Ar), 7.78 (1H, d, $J = 8.6$ Hz, H-Ar), 7.63-7.54 (2H, m, H-C(6, 7)), 3.24 (1H, qui, $J = 8.1$ Hz, H-C(1')), 2.65 (3H, s, Me-C=O), 2.23-2.11 (4H, m), 1.91-1.81 (2H, m), 1.78-1.66 (2H, m).

2-Acetylnaphthalen-1-yl cyclohex-1-ene-1-carboxylate (21). Yield: 59%, as a white powder. ^1H NMR (300 MHz, CDCl_3) δ 7.97-7.92 (1H, m, H-Ar.), 7.90-7.83 (2H, m, H-Ar.), 7.78 (1H, d, $J = 8.6$ Hz), 7.63-7.51 (2H, m), 7.45 (1H, qui, $J = 1.8$ Hz, H-C=C), 2.63 (3H, s, Me-C=O), 2.55-2.46 (2H, m), 2.42-2.32 (2H, m), 1.86-1.68 (4H, m). ^{13}C NMR (75 MHz, CDCl_3) δ 21.34, 22.03, 24.28, 26.19, 30.15, 123.06, 125.13, 125.81, 127.21, 127.33, 127.52, 127.89, 128.45, 129.59, 136.33, 143.27, 146.94, 165.71, 197.33. HRMS (ESI) calcd. for $\text{C}_{19}\text{H}_{18}\text{O}_3\text{Na}$ $[\text{M} + \text{Na}]^+$ 317.11536, found 317.11440

2-Acetylnaphthalen-1-yl bicyclo[2.2.1]hept-5-ene-2-carboxylate (22). Yield: quant, dr 4:1, as a light brown oil. ^1H NMR (300 MHz, CDCl_3) δ 8.01-7.75 (4H, m, H-Ar.), 7.64-7.54 (2H, m, H-Ar.), 6.38-6.19 (2H, m, H-C=C), 3.60-3.46 (1.8H, m), 3.09-3.01 (1H, m), 2.79-2.72 (0.2H, m), 2.65, 2.64 (1:4)(3H, s, Me-C=O), 2.29-2.13 (1H, m), 1.74-1.51 (2.2H, m), 1.48-1.42 (0.8H, m). (major-isomer) ^{13}C NMR (75 MHz, CDCl_3) δ 29.78, 29.86, 42.69, 43.98, 45.98, 49.93, 122.95, 124.97, 125.77, 126.90, 127.23, 127.51, 127.87, 128.41, 132.71, 136.17, 138.21, 146.21, 173.20, 198.16. (minor-isomer) ^{13}C NMR (75 MHz, CDCl_3) δ 29.78, 30.60, 41.82, 43.51, 46.59, 46.68, 122.83, 125.03, 125.83, 126.90, 127.35, 127.51, 127.91, 128.47, 132.71, 135.72, 138.49, 146.10, 174.56, 198.09. HRMS (ESI) calcd. for $\text{C}_{20}\text{H}_{18}\text{O}_3\text{Na}$ $[\text{M} + \text{Na}]^+$ 329.11536, found 329.11708.

2-Acetylnaphthalen-1-yl (3r,5r,7r)-adamantane-1-carboxylate (23). Yield: 75%, as a white powder. ^1H NMR (300 MHz, CDCl_3) δ 7.99-7.94 (1H, m, H-Ar), 7.90-7.85 (1H, m, H-Ar), 7.82-7.75 (2H, m, H-Ar), 7.62-7.53 (2H, m, H-Ar), 2.64 (3H, s, Me-C=O), 2.28-2.24 (6H, m, H-C(2', 8', 9')), 2.20-2.13

(3H, m, H-C(3', 5', 7')), 1.87-1.81 (6H, m, H-C(4', 6', 10')). ^{13}C NMR (75 MHz, CDCl_3) δ 28.0 (3 Carbons), 29.89, 36.48 (3 Carbons), 39.99 (3 Carbons), 41.48, 122.74, 124.97, 125.73, 127.27, 127.54, 127.89, 128.33, 136.14, 146.04, 175.65, 198.16. HRMS (ESI) calcd. for $\text{C}_{23}\text{H}_{23}\text{O}_3\text{Na}$ [$\text{M} + \text{Na}$] $^+$ 371.16231, found 371.15966.

2-Acetylnaphthalen-1-yl 4-methoxybenzoate (25a). Yield: quant, as a white powder. ^1H NMR (300 MHz, CDCl_3) δ 8.30 (2H, dt, $J = 9.0, 2.4$ Hz, H-Ar), 8.00-7.97 (1H, m, H-Ar), 7.91 (1H, d, $J = 8.7$ Hz, H-Ar), 7.90 (1H, d, $J = 7.5$ Hz, H-Ar), 7.82 (1H, d, $J = 8.5$ Hz, H-Ar), 7.61 (1H, ddd, $J = 9.6, 7.0, 1.3$ Hz, H-Ar), 7.53 (1H, ddd, $J = 9.7, 6.9, 1.3$ Hz, H-Ar), 7.07 (2H, dt, $J = 9.0, 2.4$ Hz, H-Ar), 3.94 (3H, s, Me-O), 2.63 (3H, s, Me-C=O).

2-Acetylnaphthalen-1-yl 3-methoxybenzoate (25b). Yield: 94%, as a white powder. ^1H NMR (300 MHz, CDCl_3) δ 8.02-7.89 (4H, m, H-Ar), 7.88-7.80 (2H, m, H-Ar), 7.65-7.46 (2H, m, H-Ar), 7.29-7.23 (1H, m, H-Ar), 3.91 (3H, s, Me-O), 2.64 (3H, s, Me-C=O). ^{13}C NMR (75 MHz, CDCl_3) δ 30.19, 55.58, 114.79, 120.71, 122.89, 122.98, 125.21, 126.21, 127.18, 127.35, 127.42, 127.96, 128.61, 129.94, 130.21, 136.39, 146.72, 159.93, 164.97, 197.64. HRMS (ESI) calcd. for $\text{C}_{20}\text{H}_{16}\text{O}_4\text{Na}$ [$\text{M} + \text{Na}$] $^+$ 343.09463, found 343.09605.

4.2.4. General Procedure for Naphthalene esters (method v: 18a-c, 19, 24a, 24b).

To a solution of **4a** (4.0 g, 10.74 mmol) and 1-hydroxy-2-acetonaphone in dry DCM (40 mL) was added *N,N'*-dicyclohexylcarbodiimide (4.43 g, 21.5 mmol) and 4-dimethylaminopyridine (1.57 g, 12.9 mmol) at room temperature. After being stirred for 48h, the reaction mixture was diluted with DCM and filtrated through Celite®. The filtrate was evaporated and then purified by flash chromatography on silica gel (250 g) with 30% ether/hexane to afford **18a** (4.33 g, 94%) as a white powder.

2-Acetylnaphthalen-1-yl cis-4-((tert-butyldimethylsilyl)oxy)cyclohexane-1-carboxylate (18a). Yield: 94%. ^1H NMR (300 MHz, CDCl_3) δ 8.0-7.95 (1H, m, H-Ar), 7.90-7.86 (1H, m, H-Ar), 7.83 (1H, d, $J = 8.7$ Hz, H-Ar), 7.77 (1H, d, $J = 8.7$ Hz, H-Ar), 7.64-7.54 (2H, m, H-Ar), 4.07-4.00 (1H, m, H-C(4')), 2.83 (1H, tt, $J = 10.9, 4.0$ Hz, H-C(1')), 2.64 (3H, s, Me-C=O), 2.30-2.14 (2H, m), 2.08-1.97 (2H, m), 1.88-1.78 (2H, m), 1.70-1.58 (2H, m), 0.92 (9H, s, *t*Bu-Si), 0.07 (6H, s, (Me) $_2$ -Si). ^{13}C NMR (75 MHz, CDCl_3) δ 4.8 (2 Carbons), 18.13, 23.27 (2 Carbons), 25.85 (3 Carbons), 29.88, 32.84 (2 Carbons), 42.79, 66.14, 122.85, 125.07, 125.8, 126.83, 127.33, 127.51, 127.86, 128.46, 136.22, 146.27, 173.97, 198.0. HRMS (ESI) calcd. for $\text{C}_{25}\text{H}_{34}\text{O}_4\text{SiNa}$ [$\text{M} + \text{Na}$] $^+$ 449.21240, found 449.21525.

2-Acetylnaphthalen-1-yl trans-4-((tert-butyldimethylsilyl)oxy)cyclohexane-1-carboxylate (18b). Yield: 83%, as a white solid. ^1H NMR (300 MHz, CDCl_3) δ 7.96-7.93 (1H, m, H-Ar), 7.89-7.85 (1H, m, H-Ar), 7.82 (1H, d, $J = 8.7$ Hz, H-Ar), 7.77 (1H, d, $J = 8.7$ Hz, H-Ar), 7.63-7.53 (2H, m, H-Ar), 3.69 (1H, tt, $J = 10.3, 4.3$ Hz, H-C(4')), 2.76 (1H, tt, $J = 11.6, 3.6$ Hz, H-C(1')), 2.63 (3H, s, Me-C=O), 2.40-2.33 (2H, m), 2.08-2.02 (2H, m), 1.86-1.73 (2H, m), 1.54-1.42 (2H, m), 0.92 (9H, s, *t*Bu-Si), 0.10 (6H, s, (Me) $_2$ -Si). ^{13}C NMR (75 MHz, CDCl_3) δ 4.6 (2 Carbons), 18.25, 25.93 (3 carbons), 27.26 (2

Carbons), 29.75, 34.86 (2 Carbons), 42.46, 70.51, 122.78, 125.09, 125.87, 126.58, 127.35, 127.46, 127.9, 128.52, 136.2, 146.01, 173.87, 197.93. HRMS (ESI) calcd. for $C_{25}H_{34}O_4SiNa$ $[M + Na]^+$ 449.21240, found 449.21345.

2-Acetylnaphthalen-1-yl 3-((tert-butyldimethylsilyl)oxy)cyclohexane-1-carboxylate (18c). Yield: 90%, dr 2:1, as a white solid. 1H NMR (300 MHz, $CDCl_3$) δ 7.98-7.75 (4H, m, H-Ar), 7.65-7.53 (2H, m, H-Ar), 4.26-4.18 (0.3H, m, H-C(3')), 3.78-3.64 (0.7H, m, H-C(3')), 3.30 (0.3H, tt, $J = 10.8, 3.8$ Hz, H-C(1')), 2.85 (0.7H, tt, $J = 12.3, 3.5$ Hz, H-C(1')), 2.64, 2.63 (2:1)(3H, s, Me-C(=O)), 2.52-2.41 (0.7H, m), 2.33-2.13 (1.4H, m), 2.01-1.28 (6H, m), 0.94, 0.92 (1:2)(9H, s, *t*Bu-Si), 0.11, 0.09 (2:1)(6H, s, (Me)₂-Si). (major-isomer) ^{13}C NMR (75 MHz, $CDCl_3$) δ 4.51 (2 Carbons), 18.18, 23.71, 25.90 (3 Carbons), 28.04, 29.78, 35.57, 38.14, 42.49, 70.74, 122.78, 125.07, 125.89, 126.62, 127.37, 127.44, 127.88, 128.51, 136.21, 146.06, 173.14, 197.89. (minor-isomer) ^{13}C NMR (75 MHz, $CDCl_3$) δ 4.79, (2 Carbons), 18.11, 19.74, 25.85 (3 Carbons), 28.42, 29.89, 33.14, 36.19, 38.23, 66.32, 122.78, 125.07, 125.83, 126.62, 127.28, 127.44, 127.91, 128.42, 136.21, 147.19, 174.61, 197.89. HRMS (ESI) calcd. for $C_{25}H_{34}O_4SiNa$ $[M + Na]^+$ 449.21240, found 449.21259.

2-Acetylnaphthalen-1-yl 4-(((tert-butyldimethylsilyl)oxy)methyl)cyclohexane-1-carboxylate (19). Yield: 52%, dr 4:1, as a colorless oil. 1H NMR (300 MHz, $CDCl_3$) δ 8.01-7.75 (4H, m, H-Ar), 7.64-7.52 (2H, m, H-Ar), 3.52, 3.48 (4:1)(2H, d, $J = 6.4$ Hz, -CH₂-O), 3.10 (0.8H, qui, $J = 5.0$ Hz, H-C(1')), 2.75 (0.2H, tt, $J = 12.2, 3.4$ Hz, H-C(1')), 2.64 (3H, s, Me-C(=O)), 2.44-2.19 (2H, m), 2.02-1.65 (5H, m), 1.56-1.44 (1.6H, m), 1.20-1.05 (0.4H, m), 0.92, 0.90 (1:4)(9H, s, *t*Bu-Si), 0.06, 0.05 (1:4)(6H, s, (Me)₂-Si). (major-isomer) ^{13}C NMR (75 MHz, $CDCl_3$) δ 5.31 (2 Carbons), 18.39, 25.99 (3 Carbons), 26.06 (4 Carbons), 29.74, 38.43, 41.15, 67.03, 122.84, 125.03, 125.77, 126.83, 127.32, 127.60, 127.89, 128.43, 136.19, 146.11, 173.85, 198.10. (minor-isomer) ^{13}C NMR (75 MHz, $CDCl_3$) δ 5.31 (2 Carbons), 18.39, 25.99 (3 Carbons), 28.56 (2 Carbons), 28.68 (2 Carbons), 29.85, 39.76, 41.63, 68.39, 122.84, 125.08, 125.82, 126.91, 127.60, 127.89, 128.47, 136.19, 146.11, 173.85, 198.10. HRMS (ESI) calcd. for $C_{26}H_{36}O_4SiNa$ $[M + Na]^+$ 463.22805, found 463.22667.

2-Acetylnaphthalen-1-yl 4-((tert-butoxycarbonyl)amino)benzoate (24a). Yield: 18%, as a light yellow powder. 1H NMR (300 MHz, $CDCl_3$) δ 8.28 (2H, dt, $J = 8.8, 2.2$ Hz, H-Ar), 8.00-7.95 (1H, m, H-Ar), 7.91 (1H, d, $J = 8.7$ Hz, H-Ar), 7.90 (1H, d, $J = 7.7$ Hz, H-Ar), 7.82 (1H, d, $J = 8.3$ Hz, H-Ar), 7.64-7.50 (4H, m, H-Ar), 6.76 (1H, s, H-N), 2.62 (3H, s, Me-C(=O)), 1.56 (9H, s, *t*Bu-O). ^{13}C NMR (75 MHz, $CDCl_3$) δ 28.28 (3 Carbons), 30.29, 81.49, 117.77 (2 Carbons), 122.88, 123.03, 125.18, 126.10, 127.35, 127.42, 127.44, 127.94, 128.55, 131.94 (2 Carbons), 136.39, 143.88, 146.9, 152.1, 164.61, 197.76. HRMS (ESI) calcd. for $C_{24}H_{23}O_5NNa$ $[M + Na]^+$ 428.14739, found 428.14652.

2-Acetylnaphthalen-1-yl 3-((tert-butoxycarbonyl)amino)benzoate (24b). Yield: 54%, as a white powder. 1H NMR (300 MHz, $CDCl_3$) δ 8.21 (1H, t, $J = 1.9$ Hz, H-Ar.), 8.04-7.81 (6H, m, H-Ar.), 7.66-7.49 (3H, m, H-Ar.), 6.65 (1H, br. s, H-N), 2.64 (3H, s, Me-C(=O)), 1.54 (9H, s, *t*Bu-O). ^{13}C NMR (75 MHz, $CDCl_3$) δ 28.31(3 Carbons), 30.20, 81.09, 120.12, 123.03, 124.05, 124.97, 125.21, 126.21,

127.08, 127.33, 127.42, 127.93, 128.62, 129.63, 129.68, 136.38, 139.11, 146.74, 152.56, 164.80, 197.61. HRMS (ESI) calcd. for $C_{24}H_{23}O_5NNa$ $[M + Na]^+$ 428.14739, found 428.14981.

4.2.5. General Procedure for Benzo[h]chromone Derivatives (37-47).

To a solution of potassium *tert*-butoxide (2.0 g, 11.4 mmol) in dry THF (2 mL) was added a solution of **19** (2.50 g, 5.67 mmol) in dry THF (10 mL) at room temperature. After being stirred for 30 min, the reaction mixture was quenched with ice water, diluted with DCM and then acidified with 1M hydrochloric acid. The organic layer was separated, washed with brine, dried over with $MgSO_4$, and evaporated. The slurry was diluted with DCM, through to a pad of silica gel (15 g) with 30% AcOEt/hexane and evaporated. This crude product was immediately used in further cyclization reaction.

To a solution of the crude product (2.26 g) in dry ethanol (28 mL) was slowly added concentrated sulfuric acid (1.1 mL) at room temperature. After stirred at 80 °C for 30 min, the reaction mixture was cooled to 0 °C, neutralized with sodium hydrogen carbonate and concentrated. The slurry was diluted with DCM, and then the organic layer was separated, washed with brine, dried over with $MgSO_4$ and evaporated. The residue was purified by MPLC (SNAP Ultra 50 g, 25 μ m, 25 mL/min, 80% AcOEt/hexane) to afford **41** (1.29 g, 74%, 3 steps) as a white powder.

2-Ayclohexyl-4H-benzo[h]chromen-4-one (37). Yield: 39%, 2 steps, as a white powder. 1H NMR (300 MHz, $CDCl_3$) δ 8.53-8.48 (1H, m, H-C(10)), 8.14 (1H, d, $J = 8.7$ Hz, H-C(5)), 7.96-7.90 (1H, m, H-C(7)), 7.75 (1H, d, $J = 8.5$ Hz, H-C(6)), 7.73-7.64 (2H, m, H-C(8, 9)), 6.34 (1H, s, H-C(3)), 2.71 (1H, dt, $J = 11.5, 3.3$ Hz, H-C(1')), 2.21-2.11 (2H, m), 2.0-1.89 (2H, m), 1.88-1.77 (1H, m), 1.69-1.24 (4H, m).

2-(4-Methylcyclohexyl)-4H-benzo[h]chromen-4-one (38). Yield. 50%, 2 steps, *cis:trans* = 3:1, as a white powder. 1H NMR (300 MHz, $CDCl_3$) δ 8.50-8.45 (1H, m, H-Ar), 8.14, 8.13 (3:1)(1H, d, $J = 8.7$ Hz, H-Ar), 7.94-7.91 (1H, m, H-Ar), 7.75, 7.74 (3:1)(1H, d, $J = 8.7$ Hz, H-Ar), 6.42, 6.34 (3:1) (1H, s, H-C(3')), 2.82, 2.64 (3:1)(1H, qui, $J = 4.1$ Hz), 2.64 (0.25H, tt, $J = 12.1, 1.7$ Hz), 2.20-2.00 (2H, m), 1.94-1.83 (2.75H, m), 1.75-1.60 (2H, m), 1.57-1.45 (1.75H, m), 1.21-1.86 (0.5H, m), 1.01, 0.98 (3:1)(3H, d, $J = 6.8$ Hz, $J = 6.4$ Hz, Me-C(4')). (*cis*-isomer) ^{13}C NMR (75 MHz, $CDCl_3$) δ 19.45, 26.02 (2 Carbons), 28.96 31.01 (2 Carbons), 40.59, 110.11, 119.9, 120.83, 122.21, 124.08, 124.92, 127.01, 128.16, 129.10, 135.84, 153.84, 171.77, 178.52. (*trans*-isomer) ^{13}C NMR (75 MHz, $CDCl_3$) δ 22.48, 30.71 (2 Carbons), 32.19, 34.58 (2 Carbons), 42.56, 109.23, 119.97, 120.83, 122.21, 124.07, 124.88, 126.97, 128.14, 129.1, 135.84, 153.76, 172.41, 178.58. HRMS (ESI) calcd. for $C_{20}H_{21}O_2$ $[M + H]^+$ 293.15415, found 293.15149.

2-(4-Isopropylcyclohexyl)-4H-benzo[h]chromen-4-one (39). Yield: 84%, 2 steps, *cis:trans* = 4:1, as a white powder. 1H NMR (300 MHz, $CDCl_3$) δ 8.51-8.46 (1H, m, H-C(10)), 8.15, 8.14 (4:1)(1H, d, $J = 8.7$ Hz, H-C(5)), 7.95-7.91 (1H, m, H-C(7)), 7.76, 7.75 (4:1)(1H, d, $J = 8.9$ Hz, H-C(6)), 7.71-7.65 (2H, m), 6.45, 6.34 (4:1) (1H, s, H-C(3)), 3.00 (0.8H, qui, $J = 5.4$ Hz, H-C(1')), 2.63 (0.2H, tt, $J = 12.2,$

3.4 Hz, H-C(1')), 2.25-2.05 (2H, m), 1.98-1.79 (2.4H, m), 1.69-1.50 (4H, m), 1.30-1.16 (1.6H, m), 0.93, 0.89 (1:4)(6H, d, $J = 6.8$ Hz, (Me)₂-CH). (*cis*-isomer) ¹³C NMR (75 MHz, CDCl₃) δ 20.39 (2 Carbons), 26.45 (2 Carbons), 26.92 (2 Carbons), 29.82, 39.62, 42.24, 110.50, 119.87, 120.83, 122.23, 124.09, 124.92, 127.02, 128.16, 129.09, 153.86, 171.43, 178.43. (*trans*-isomer) ¹³C NMR (75 MHz, CDCl₃) δ 19.80 (2 Carbons), 29.21 (2 Carbons), 30.89 (2 Carbons), 32.79, 42.98, 43.44, 109.23, 119.99, 120.83, 122.23, 124.09, 124.86, 126.96, 128.16, 129.09, 153.74, 172.38, 178.55. HRMS (ESI) calcd. for C₂₂H₂₅O₂ [M + H]⁺ 321.18545, found 321.18470.

2-(*cis*-4-Hydroxycyclohexyl)-4H-benzo[h]chromen-4-one (40a). Yield: 30%, 3 steps, as a white powder. ¹H NMR (300 MHz, CDCl₃) δ 8.53-8.49 (1H, m, H-C(10)), 8.14 (1H, d, $J = 8.7$ Hz, H-C(5)), 7.95-7.91 (1H, m, H-C (7)), 7.76 (1H, d, $J = 8.7$ Hz, H-C(6)), 7.73-7.64 (2H, m, H-C(8, 9)), 6.38 (1H, s, H-C(3)), 4.21-4.16 (1H, m, H-C(4')), 2.77 (1H, tt, $J = 11.2, 3.4$ Hz, H-C(1')), 2.21-2.08 (2H, m), 2.01-1.92 (4H, m), 1.82-1.70 (2H, m), 1.42 (1H, s, OH). ¹³C NMR (75 MHz, CDCl₃) δ 24.51 (2 Carbons), 32.31 (2 Carbons), 41.97, 65.34, 109.57, 120.0, 120.84, 122.35, 124.1, 125.06, 127.12, 128.2, 129.24, 135.91, 153.88, 171.91, 178.67. HRMS (ESI) calcd. for C₁₉H₁₉O₃ [M + H]⁺ 295.13342, found 295.13598.

2-(*trans*-4-Hydroxycyclohexyl)-4H-benzo[h]chromen-4-one (40b). Yield: 47%, 3 steps, as a white powder. ¹H NMR (300 MHz, CDCl₃) δ 8.49-8.46 (1H, m, H-C(10)), 8.13 (1H, d, $J = 8.7$ Hz, H-C(5)), 7.95-7.92 (1H, m, H-C(7)), 7.76 (1H, d, $J = 8.7$ Hz, H-C(6)), 7.74-7.65 (2H, m, H-C(8, 9)), 6.35 (1H, s, H-C(3)), 3.77 (1H, dt, $J = 10.7, 4.1$ Hz, H-C(4')), 2.70 (1H, dt, $J = 12.0, 3.2$ Hz, H-C(1')), 2.32-2.15 (4H, m), 1.80-1.62 (2H, m), 1.59-1.43 (3H, m). ¹³C NMR (75 MHz, CDCl₃) δ 28.64 (2 Carbons), 34.91 (2 Carbons), 41.7, 69.94, 109.48, 119.98, 120.8, 122.15, 123.99, 125.05, 127.06, 128.2, 129.19, 135.88, 153.74, 171.2, 178.4. HRMS (ESI) calcd. for C₁₉H₁₉O₃ [M + H]⁺ 295.13342, found 295.13440.

2-(*cis*-3-hydroxycyclohexyl)-4H-benzo[h]chromen-4-one (40c). Yield: 59%, 3 steps, as a white powder. ¹H NMR (300 MHz, CDCl₃) δ 8.50-8.47 (1H, m, H-C(10)), 8.14 (1H, d, $J = 8.7$ Hz, H-C(5)), 7.95-7.92 (1H, m, H-C (7)), 7.76 (1H, d, $J = 8.7$ Hz, H-C(6)), 7.74-7.65 (2H, m, H-C(8, 9)), 6.35 (1H, s, H-C(3)), 3.82 (1H, tt, $J = 10.8, 4.2$ Hz, H-C(3')), 2.77 (1H, tt, $J = 12.1, 3.2$ Hz, H-C(1')), 2.49-2.41 (2H, m), 2.17-2.09 (2H, m), 2.05-1.99 (1H, m), 1.79-1.70 (1H, m, H-O), 1.68-1.57 (2H, m), 1.57-1.49 (2H, m), 1.46-1.31 (1H, m). ¹³C NMR (75 MHz, CDCl₃) δ 23.81, 29.74, 35.14, 39.31, 41.38, 70.13, 109.49, 119.99, 120.8, 122.18, 123.99, 125.06, 127.06, 128.18, 129.2, 135.88, 153.73, 170.57, 178.45. HRMS (ESI) calcd. for C₁₉H₁₈O₃Na [M + Na]⁺ 317.11536, found 317.11516.

2-(*trans*-3-Hydroxycyclohexyl)-4H-benzo[h]chromen-4-one (40d). Yield: 59%, as a white powder. ¹H NMR (300 MHz, CDCl₃) δ 8.51-8.48 (1H, m, H-C(10)), 8.14 (1H, d, $J = 8.7$ Hz, H-C(5)), 7.95-7.92 (1H, m, H-C (7)), 7.76 (1H, d, $J = 8.7$ Hz, H-C(6)), 7.73-7.65 (2H, m, H-C(8, 9)), 6.36 (1H, s, H-C(3)), 4.36-4.32 (1H, m, H-C(3')), 2.77 (1H, tt, $J = 11.8, 3.6$ Hz, H-C(1')), 2.25-2.14 (2H, m), 1.96-1.84 (3H, m), 1.78-1.60 (3H, m). ¹³C NMR (75 MHz, CDCl₃) δ 19.66, 30.16, 32.39, 36.69, 36.81, 65.78, 109.53, 119.95, 120.79, 122.21, 124.01, 124.96, 127.01, 128.14, 129.14, 135.84, 153.78, 172.06,

178.52. HRMS (ESI) calcd. for $C_{19}H_{18}O_3Na$ $[M + Na]^+$ 317.11536, found 317.11516.

2-(4-(Hydroxymethyl)cyclohexyl)-4H-benzo[h]chromen-4-one (41). Yield: 74%, 3 steps, *cis:trans* = 1:1, as a white powder. 1H NMR (300 MHz, $CDCl_3$) δ 8.52-8.44 (1H, m, H-C(10)), 8.13 (1H, d, J = 8.7 Hz, H-C(5)), 7.96-7.90 (1H, m, H-C(7)), 7.75 (1H, d, J = 8.7 Hz, H-C(6)), 7.73-7.64 (2H, m, H-C(8, 9)), 6.41, 6.35 (1:1)(1H, s, H-C(3)), 3.65, 3.57 (1:1)(2H, d, CH_2 -OH), 2.96 (0.5H, qui, J = 3.9 Hz, H-C(1')), 2.69 (0.5H, dt, J = 12.1, 3.4 Hz, H-C(1')), 2.31-2.20 (1H, m), 2.11-1.86 (3.5H, m), 1.81-1.60 (4.5H, m), 1.29-1.16 (1H, m). (*cis:trans* = 1:1) ^{13}C NMR (75 MHz, $CDCl_3$) δ 25.77, 26.29, 28.88, 30.12, 37.25 (0.5C), 39.88 (0.5C), 40.34 (0.5C), 42.79 (0.5C), 65.46 (0.5C), 68.18 (0.5C), 109.31 (0.5C), 110.26 (0.5C), 119.89 (0.5C), 119.98 (0.5C), 120.08, 122.18, 124.04, 124.95 (0.5C), 125.01 (0.5C), 127.01 (0.5C), 127.07 (0.5C), 128.18, 129.14, 135.85, 153.82, 171.24 (0.5C), 171.96 (0.5C), 178.43 (0.5C), 178.53 (0.5C). HRMS (ESI) calcd. for $C_{20}H_{21}O_3$ $[M + H]^+$ 309.14907, found 309.15127.

2-Cyclopentyl-4H-benzo[h]chromen-4-one (42). Yield: 95%, 2 steps, as a white powder. 1H NMR (300 MHz, $CDCl_3$) δ 8.49-8.44 (1H, m, H-C(10)), 8.14 (1H, d, J = 8.7 Hz, H-C(5)), 7.96-7.91 (1H, m, H-C(7)), 7.76 (1H, d, J = 8.5 Hz, H-C(6)), 7.73-7.64 (2H, m, H-C(8, 9)), 6.38 (1H, s, H-C(3)), 3.26-3.12 (1H, m, H-C(1')), 2.26-2.13 (2H, m), 2.02-1.86 (4H, m), 1.85-1.73 (2H, m).

2-(Cyclohex-1-en-1-yl)-4H-benzo[h]chromen-4-one (43). Yield: 29%, 2 steps, as a white powder. 1H NMR (300 MHz, $CDCl_3$) δ 8.54-8.50 (1H, m, H-C(10)), 8.14 (1H, d, J = 8.7 Hz, H-C(5)), 7.95-7.92 (1H, m, H-C(7)), 7.75 (1H, d, J = 8.7 Hz, H-C(6)), 7.73-7.65 (2H, m, H-C(8, 9)), 7.18-7.15 (1H, m, H-C=C), 6.47 (1H, s, H-C(3)), 2.44-2.40 (4H, m), 1.89-1.82 (2H, m), 1.78-1.72 (2H, m). ^{13}C NMR (75 MHz, $CDCl_3$) δ 21.62, 22.19, 24.28, 26.11, 107.32, 119.99, 120.82, 122.38, 124.20, 124.82, 126.93, 128.18, 129.06, 129.96, 133.58, 136.0, 153.23, 163.04, 178.79. HRMS (ESI) calcd. for $C_{19}H_{17}O_2$ $[M + H]^+$ 277.12285, found 277.12243.

2-((2S)-Bicyclo[2.2.1]hept-5-en-2-yl)-4H-benzo[h]chromen-4-one (exo-44). Yield: 39%, 2 steps, as a white powder. 1H NMR (300 MHz, $CDCl_3$) δ 8.48-8.43 (1H, m, H-C(10)), 8.15 (1H, d, J = 8.7 Hz, H-C(5)), 7.96-7.92 (1H, m, H-C(7)), 7.76 (1H, d, J = 8.7 Hz, H-C(6)), 7.74-7.67 (2H, m, H-C(8, 9)), 6.44 (1H, s, H-C(3)), 6.33-6.26 (2H, m, H-C=C-H), 3.20 (1H, s), 3.12 (1H, s), 2.74 (1H, dd, J = 8.9, 4.7 Hz), 2.05-1.99 (1H, m), 1.79 (1H, d, J = 8.9 Hz), 1.76-1.65 (1H, m), 1.65-1.57 (1H, m). ^{13}C NMR (75 MHz, $CDCl_3$) δ 31.67, 42.08, 43.41, 46.67, 47.14, 110.42, 119.96, 120.85, 122.25, 124.02, 125.01, 127.05, 128.2, 129.11, 135.88, 136.36, 138.13, 153.92, 171.71, 178.34. HRMS (ESI) calcd. for $C_{20}H_{17}O_2$ $[M + H]^+$ 289.12285, found 289.12381.

2-((1S,2S,4S)-Bicyclo[2.2.1]hept-5-en-2-yl)-4H-benzo[h]chromen-4-one (endo-44). Yield: 39%, 2 steps, as a white powder. 1H NMR (300 MHz, $CDCl_3$) δ 8.48-8.45 (1H, m, H-C(10)), 8.12 (1H, d, J = 8.7 Hz, H-C(5)), 7.95-7.90 (1H, m, H-C(7)), 7.74 (1H, d, J = 8.9 Hz, H-C(6)), 7.71-7.64 (2H, m, H-C(8, 9)), 6.35 (1H, dd, J = 5.7, 3.0 Hz, H-C=C), 6.25 (1H, s, H-C(3)), 5.95 (1H, dd, J = 5.7, 2.8 Hz, H-C=C), 3.49 (1H, dt, J = 13.3, 4.3), 3.42 (1H, s), 3.08 (1H, s), 2.26 (1H, ddd, J = 12.4, 9.3, 3.7 Hz), 1.63 (1H, ddd, J = 8.3, 4.0, 1.9 Hz), 1.52 (1H, d, J = 8.3 Hz), 1.51-1.53 (1H, m). ^{13}C NMR (75 MHz,

CDCl₃) δ 30.86, 42.92, 43.0, 47.34, 50.05, 110.8, 119.94, 120.83, 122.31, 124.08, 127.0, 128.13, 129.06, 132.36, 135.81, 138.0, 153.72, 170.91, 178.19. HRMS (ESI) calcd. for C₂₀H₁₇O₂ [M + H]⁺ 289.12285, found 289.12381.

2-((3*r*,5*r*,7*r*)-Adamantan-1-yl)-4*H*-benzo[*h*]chromen-4-one (45). Yield: 63%, 2 steps, as a white powder. ¹H NMR (300 MHz, CDCl₃) δ 8.53-8.48 (1H, m, H-C(10)), 8.13 (1H, d, *J* = 8.7 Hz, H-C(5)), 7.95-7.91 (1H, m, H-C(7)), 7.75 (1H, d, *J* = 8.9 Hz, H-C(6)), 7.72-7.66 (2H, m, H-C(8, 9)), 6.36 (1H, s, H-C(3)), 2.21-2.17 (3H, m, H-C(3', 5', 7')), 2.12-2.09 (6H, m, H-C(2', 8', 9')), 1.91-1.81 (6H, m, H-C(4', 6', 10')). ¹³C NMR (75 MHz, CDCl₃) δ 28.05 (3 Carbons), 36.5 (3 Carbons), 38.49, 40.05 (3 Carbons), 107.92, 119.8, 120.85, 122.2, 124.22, 124.8, 127.0, 128.18, 129.09, 135.85, 153.68, 174.86, 178.88. HRMS (ESI) calcd. for C₂₃H₂₃O₂ [M + H]⁺ 331.16980, found 331.17209.

2-(4-Aminophenyl)benzo[*h*]chromen-4-one (46a). Yield: 77%, 3 steps, as a light yellow powder. ¹H NMR (300 MHz, CDCl₃) δ 8.65-8.61 (1H, m, H-C(10)), 8.19 (1H, d, *J* = 8.7 Hz, H-C(5)), 7.99-7.93 (1H, m, H-C(7)), 7.88 (2H, dt, *J* = 8.8, 2.3 Hz), 7.78 (1H, d, *J* = 8.7 Hz, H-C(6)), 7.74-7.69 (2H, m), 6.85 (1H, s, H-C(3)), 6.83 (2H, dt, *J* = 8.7, 2.3 Hz), 4.12 (2H, s, H₂N).

2-(3-Aminophenyl)-4*H*-benzo[*h*]chromen-4-one (46b). Yield: 36%, 3 steps, as a light yellow powder. ¹H NMR (300 MHz, DMSO-*d*) δ 8.76-8.69 (1H, m), 8.20-8.13 (1H, m), 8.02 (1H, d, *J* = 8.7 Hz), 7.96 (1H, d, *J* = 8.7 Hz), 7.88-7.83 (2H, m), 7.47 (1H, t, *J* = 2.0 Hz), 7.37-7.31 (1H, m), 7.24 (1H, t, *J* = 7.8 Hz), 7.01 (1H, s), 6.84-6.79 (1H, m), 5.51 (2H, br. s, H₂N).

2-(4-Methoxyphenyl)-4*H*-benzo[*h*]chromen-4-one (47a). Yield: 77%, 2 steps, as a white powder. ¹H NMR (300 MHz, CDCl₃) δ 8.66-8.60 (1H, m, H-C(10)), 8.19 (1H, d, *J* = 8.7 Hz, H-C(5)), 8.01 (2H, dt, *J* = 9.0, 2.5 Hz, H-C(2', 6')), 7.98-7.95 (1H, m, H-C(7)), 7.80 (1H, d, *J* = 8.7 Hz, H-C(6)), 7.75-7.70 (2H, m, H-C(8, 9)), 7.10 (2H, dt, *J* = 9.1, 2.5 Hz, H-C(3', 4')), 6.91 (1H, s, H-C(3)), 3.93 (3H, s, Me-O).

2-(3-Methoxyphenyl)-4*H*-benzo[*h*]chromen-4-one (47b). Yield: 80%, 2 steps, as a brown powder. ¹H NMR (300 MHz, CDCl₃) δ 8.66-8.61 (1H, m, H-C(10)), 8.20 (1H, d, *J* = 8.7 Hz, H-C(5)), 7.99-7.95 (1H, m, H-C(7)), 7.82 (1H, d, *J* = 8.5 Hz, H-C(6)), 7.76-7.72 (2H, m, H-C(8, 9)), 7.66-7.62 (1H, m, H-Ar), 7.56 (1H, t, *J* = 2.0 Hz, H-Ar), 7.50 (1H, m, H-Ar), 7.16-7.10 (1H, m, H-Ar), 6.98 (1H, s, H-C(3)), 3.95 (3H, s, Me-O).

4.2.6. General Procedure for Mesylated Compounds (48a-d, 54).

To a solution of **40a** (542 mg, 1.84 mmol) in DCM (6 mL) was added triethylamine (308 mL, 2.21 mmol) and methanesulfonyl chloride (171 mL, 2.21 mmol) at 0 °C. After being stirred for 45 min, the reaction mixture was quenched with ice water and diluted with DCM. The organic layer was separated, washed with brine, dried over MgSO₄ and evaporated. The residue was purified by chromatography on silica gel (10 g) with 50% AcOEt/hexane to afford **48a** (607 mg, 88%) as a white powder.

cis-4-(4-oxo-4*H*-Benzo[*h*]chromen-2-yl)cyclohexyl methanesulfonate (48a). ¹H NMR (300 MHz,

CDCl₃) δ 8.50-8.44 (1H, m, H-C(10)), 8.13 (1H, d, J = 8.7 Hz, H-C(5)), 7.96-7.91 (1H, m, H-C (7)), 7.76 (1H, d, J = 8.7 Hz, H-C(6)), 7.74-7.66 (2H, m, H-C(8, 9)), 6.37 (1H, s, H-C(3)), 5.15-5.10 (1H, m, H-C(4')), 3.09 (3H, s, Me-S(=O)₂), 2.88-2.75 (1H, m, H-C(1')), 2.37-2.25 (2H, m), 2.13-1.99 (4H, m), 1.91-1.78 (2H, m). ¹³C NMR (75 MHz, CDCl₃) δ 24.39(2 Carbons), 30.56 (2 Carbons), 38.77, 41.03, 77.03, 109.65, 120.0, 120.77, 122.11, 123.96, 125.13, 127.14, 128.21, 129.23, 135.9, 153.71, 170.53, 178.28. HRMS (ESI) calcd. for C₁₉H₁₉O₃ [M + H]⁺ 295.13342, found 295.13598.

trans-4-(4-oxo-4H-Benzo[h]chromen-2-yl)cyclohexyl methanesulfonate (48b). Yield: 98%, as a white powder. ¹H NMR (300 MHz, CDCl₃) δ 8.49-8.43 (1H, m, H-C(10)), 8.13 (1H, d, J = 8.7 Hz, H-C(5)), 7.97-7.92 (1H, m, H-C (7)), 7.76 (1H, d, J = 8.8 Hz, H-C(6)), 7.75-7.66 (2H, m, H-C(8, 9)), 6.34 (1H, s, H-C(3)), 4.77 (1H, sep, J = 4.9 Hz, H-C(4')), 3.08 (3H, s, Me-S(=O)₂) 2.79-2.69 (1H, m, H-C(1')), 2.42-2.28 (4H, m), 1.88-1.74 (4H, m). ¹³C NMR (75 MHz, CDCl₃) δ 28.48 (2 Carbons), 32.15 (2 Carbons), 38.87, 40.12, 79.69, 109.78, 120.0, 120.75, 122.05, 123.91, 125.19, 127.16, 128.24, 129.28, 135.9, 153.68, 169.86, 178.21. HRMS (ESI) calcd. for C₂₀H₂₀O₅SNa [M + Na]⁺ 395.09291, found 395.09131.

cis-3-(4-oxo-4H-Benzo[h]chromen-2-yl)cyclohexyl methanesulfonate (48c). Yield: 99%, as a white powder. ¹H NMR (300 MHz, CDCl₃) δ 8.47-8.44 (1H, m, H-C(10)), 8.12 (1H, d, J = 8.7 Hz, H-C(5)), 7.96-7.91 (1H, m, H-C (7)), 7.76 (1H, d, J = 8.7 Hz, H-C(6)), 7.74-7.66 (2H, m, H-C(8, 9)), 6.34 (1H, s, H-C(3)), 4.83 (1H, tt, J = 11.0, 4.4 Hz, H-C(3')), 3.07 (3H, s, Me-S(=O)₂), 2.85 (1H, tt, J = 12.1, 3.4 Hz, H-C(1')), 2.68-2.60 (1H, m), 2.36-2.30 (1H, m), 2.16-2.69 (2H, m), 1.96-1.84 (1H, m), 1.72-1.55 (3H, m). ¹³C NMR (75 MHz, CDCl₃) δ 19.76, 23.48, 29.21, 32.48, 36.59, 36.76, 38.98, 41.19, 79.47, 109.76, 119.99, 120.7, 122.1, 123.88, 125.24, 127.19, 128.21, 129.3, 135.91, 153.66, 169.13, 178.19. HRMS (ESI) calcd. for C₂₀H₂₀O₅SNa [M + Na]⁺ 395.09291, found 395.09217.

trans-3-(4-oxo-4H-Benzo[h]chromen-2-yl)cyclohexyl methanesulfonate (48d). Yield: 92%, as a white powder. ¹H NMR (300 MHz, CDCl₃) δ 8.49-8.46 (1H, m, H-C(10)), 8.13 (1H, d, J = 8.7 Hz, H-C(5)), 7.96-7.92 (1H, m, H-C (7)), 7.77 (1H, d, J = 8.5 Hz, H-C(6)), 7.74-7.66 (2H, m, H-C(8, 9)), 6.35 (1H, s, H-C(3)), 5.26-5.22 (1H, m, H-C(3')), 3.26-3.16 (1H, m, H-C(1')), 3.11 (3H, s, Me-S(=O)₂), 2.59-2.51 (1H, m), 2.27-2.17 (2H, m), 2.01-1.95 (1H, m), 1.92-1.86 (2H, m), 1.77-1.64 (2H, m). ¹³C NMR (75 MHz, CDCl₃) δ 19.76, 29.6, 30.47, 34.94, 36.76, 38.78, 109.73, 119.99, 120.75, 122.13, 123.94, 125.17, 127.17, 128.2, 129.26, 135.9, 153.72, 170.36, 178.25. HRMS (ESI) calcd. for C₂₀H₂₁O₅SH [M + H]⁺ 373.11097, found 373.11075.

(4-(4-oxo-4H-Benzo[h]chromen-2-yl)cyclohexyl)methyl methanesulfonate (54). Yield: 93%, dr 1:1, as a amorphous. ¹H NMR (300 MHz, CDCl₃) δ 8.49-8.44 (1H, m, H-C(10)), 8.14, 8.13 (1:1)(1H, d, J = 8.7 Hz, H-C(5)), 7.96-7.91 (1H, m, H-C(7)), 7.76, 7.75 (1:1)(1H, d, J = 8.7 Hz, H-C(6)), 7.74-7.65 (2H, m, H-C(8, 9)), 6.41, 6.34 (1:1)(1H, s, H-C(3)), 4.20, 4.14 (1:1)(2H, d, J = 7.4 Hz, CH₂-O), 3.05, 3.03 (1:1)(3H, s, Me-S(=O)₂), 3.02-2.96 (0.5H, m, H-C(1')), 2.70 (0.5H, dt, J = 12.1, 3.3 Hz, H-C(1')), 2.32-2.22 (1H, m), 2.18-1.58 (7H, m), 1.37-1.23 (1H, m). ¹³C NMR (75 MHz, CDCl₃) δ 25.39,

25.99, 28.48, 29.69, 34.5(0.5C), 36.95 (0.5C), 37.39, 39.68 (0.5C), 42.36 (0.5C), 71.98 (0.5C), 73.99 (0.5C), 109.44 (0.5C), 110.43 (0.5C), 120.0, 120.75 (0.5C), 120.79 (0.5C), 122.13, 123.99, 125.03 (0.5C), 125.12 (0.5C), 127.06 (0.5C), 127.17 (0.5C), 129.18 (0.5C), 129.22 (0.5C), 135.86, 153.71 (0.5C), 153.8 (0.5C), 170.42 (0.5C), 171.25 (0.5C), 178.26 (0.5C), 178.39 (0.5C). HRMS (ESI) calcd. for $C_{21}H_{22}O_5SNa$ $[M + Na]^+$ 409.10856, found 409.10905.

4.2.7. General Procedure for Azide-containing Compounds (49a-c, 55).

To a solution of **48b** (162 mg, 0.434 mmol) in dry DMF (3 mL) was added sodium azide (141 mg, 2.17 mmol) at room temperature. After being stirred for 10 h at 80 °C, the reaction mixture was cooled to room temperature, and then quenched with ice water and diluted with 50% AcOEt/hexane. The organic layer was separated, washed with brine, dried over $MgSO_4$, and evaporated. The residue was purified by MPLC (SNAP Ultra 10 g, 25 μ m, 10 mL/min, 40% ether/hexane) to afford **49a** (112 mg, 81%) as a white powder, **49b** (18 mg, 13%) as a white powder and **50** (7.2 mg, 6%) as a white powder.

2-(cis-4-Azidocyclohexyl)-4H-benzo[h]chromen-4-one (49a). 1H NMR (300 MHz, $CDCl_3$) δ 8.52-8.46 (1H, m, H-C(10)), 8.13 (1H, d, $J = 8.7$ Hz, H-C(5)), 7.97-7.91 (1H, m, H-C(7)), 7.76 (1H, d, $J = 8.7$ Hz, H-C(6)), 7.74-7.66 (2H, m, H-C(8, 9)), 6.36 (1H, s, H-C(3)), 4.0 (1H, qui, $J = 3.3$ Hz, H-C(4')), 2.76 (1H, qui, $J = 7.3$ Hz, H-C(1')), 2.12-1.96 (6H, m), 1.86-1.70 (2H, m). ^{13}C NMR (75 MHz, $CDCl_3$) δ 24.88 (2 Carbons), 29.25 (2 Carbons), 41.54, 56.77, 109.68, 120.0, 120.8, 122.17, 124.01, 125.07, 127.11, 128.18, 129.19, 135.89, 153.74, 170.87, 178.37. HRMS (ESI) calcd. for $C_{19}H_{18}N_3O_2$ $[M + H]^+$ 320.13990, found 320.14193.

2-(trans-4-Azidocyclohexyl)-4H-benzo[h]chromen-4-one (49b). 1H NMR (300 MHz, $CDCl_3$) δ 8.49-8.43 (1H, m, H-C(10)), 8.13 (1H, d, $J = 8.7$ Hz, H-C(5)), 7.97-7.91 (1H, m, H-C(7)), 7.76 (1H, d, $J = 8.7$ Hz, H-C(6)), 7.74-7.65 (2H, m, H-C(8, 9)), 6.34 (1H, s, H-C(3)), 3.44 (1H, tt, $J = 11.3, 4.2$ Hz, H-C(4')), 2.72 (1H, tt, $J = 11.7, 3.4$ Hz, H-C(1')), 2.35-2.18 (4H, m), 1.82-1.49 (4H, m). ^{13}C NMR (75 MHz, $CDCl_3$) δ 28.95 (2 Carbons), 31.18 (2 Carbons), 41.44, 59.25, 109.59, 120.0, 120.79, 122.07, 123.96, 125.13, 127.1, 128.24, 129.24, 135.91, 153.71, 170.53, 178.3. HRMS (ESI) calcd. for $C_{19}H_{18}N_3O_2$ $[M + H]^+$ 320.13990, found 320.14400.

2-(Cyclohex-3-en-1-yl)-4H-benzo[h]chromen-4-one (50). 1H NMR (300 MHz, $CDCl_3$) δ 8.51-8.47 (1H, m, H-C(10)), 8.15 (1H, d, $J = 8.7$ Hz, H-C(5)), 7.96-7.93 (1H, m, H-C(7)), 7.76 (1H, d, $J = 8.8$ Hz, H-C(6)), 7.74-7.65 (2H, m, H-C(8, 9)), 6.39 (1H, s, H-C(3)), 5.84-5.82 (2H, m, H-C=C-H), 3.06-2.97 (1H, m, H-C(1')), 2.57-2.42 (2H, m), 2.29-2.19 (3H, m), 2.01-1.89 (1H, m). ^{13}C NMR (75 MHz, $CDCl_3$) δ 24.76, 26.4, 29.37, 38.8, 109.66, 120.01, 120.84, 122.21, 124.05, 124.97, 125.04, 127.02, 127.1, 128.16, 129.13, 135.86, 153.8, 171.7, 178.45. HRMS (ESI) calcd. for $C_{19}H_{17}O_2$ $[M + H]^+$ 277.12285, found 277.12680.

2-(3-Azidocyclohexyl)-4H-benzo[h]chromen-4-one (49c). Yield: 87 %, dr 1:1, as a white powder. 1H NMR (300 MHz, $CDCl_3$) δ 8.49-8.45 (1H, m, H-C(10)), 8.13 (1H, d, $J = 8.7$ Hz, H-C(5)), 7.95-

7.92 (1H, m, H-C (7)), 7.78-7.74 (1H, m, H-C(6)), 7.74-7.65 (2H, m, H-C(8, 9)), 6.35, 6.34 (each 0.5 H, s, H-C(3)), 4.16-4.12 (0.5 H, m, H-C(4')), 3.50 (0.5 H, tt, $J = 11.5, 4.1$ Hz), 3.10 (0.5 H, tt, $J = 11.6, 3.5$ Hz, H-C(1')), 2.80 (0.5 H, tt, $J = 12.0, 3.4$ Hz, H-C(1')), 2.51-2.40 (0.5H, m), 2.30-1.75 (5H, m), 1.74-1.36 (2.5H, m). ^{13}C NMR (75 MHz, CDCl_3) (1:1 mixture) δ 20.22, 24.03, 29.09, 29.49, 29.72, 31.24, 33.99, 35.74, 37.08, 41.49, 57.08, 59.37, 109.64, 109.66, 119.97, 120.01, 120.76, 120.77, 122.10, 122.13, 123.93, 123.96, 125.08, 125.16, 127.11, 127.13, 128.19, 128.21, 129.2, 129.25, 135.88, 135.9, 153.69, 153.72, 169.84, 170.93, 178.28, 178.31. HRMS (ESI) calcd. for $\text{C}_{19}\text{H}_{18}\text{N}_3\text{O}_2$ $[\text{M} + \text{H}]^+$ 320.13990, found 320.14385.

2-(4-(Azidomethyl)cyclohexyl)-4H-benzo[h]chromen-4-one (55). Yield: 97%, *cis:trans* = 2:3, as a white powder. ^1H NMR (300 MHz, CDCl_3) δ 8.51-8.45 (1H, m, H-C(10)), 8.15, 8.14 (2:3)(1H, d, $J = 8.7$ Hz, H-C(5)), 7.97-7.91 (1H, m, H-C(7)), 7.77, 7.76 (2:3)(1H, d, $J = 8.9$ Hz, H-C(6)), 7.74-7.65 (2H, m, H-C(8, 9)), 6.41, 6.34 (2:3)(1H, s, H-C(3)), 3.31, 3.25 (2:3)(2H, d, $J = 7.4$ Hz, $\text{CH}_2\text{-N}_3$), 3.03-2.95 (0.4H, m, H-C(1')), 2.69 (0.75H, dt, $J = 12.0, 3.4$ Hz, H-C(1')), 2.30-2.20 (1.2H, m), 2.15-1.60 (7H, m), 1.32-1.18 (0.8H, m). (*trans*-isomer) ^{13}C NMR (75 MHz, CDCl_3) δ 26.12, 26.63, 29.87, 29.99, 35.52, 42.49, 57.56, 109.41, 120.01, 120.82, 122.14, 124.02, 124.99, 127.03, 128.18, 129.15, 135.86, 153.72, 171.49, 178.43. (*cis*-isomer) ^{13}C NMR (75 MHz, CDCl_3) δ 26.12, 26.63, 29.87, 29.99, 34.93, 39.8, 55.03, 110.41, 119.91, 120.82, 122.14, 124.02, 125.07, 127.11, 128.22, 129.15, 135.86, 153.82, 170.68, 178.3. HRMS (ESI) calcd. for $\text{C}_{20}\text{H}_{20}\text{N}_3\text{O}_2$ $[\text{M} + \text{H}]^+$ 334.15555, found 334.15308.

4.2.8. General Procedure for Amine-containing Compounds 51a-c.

To a solution of **49a** (55.4 mg, 0.174 mmol) in 75% MeOH/THF (3 mL) was added nickel(II) chloride hexahydrate (66.0 mg, 0.278 mmol) at 0 °C and then slowly added sodium borohydride (30.2 mg, 0.799 mmol). After being stirred 4 h at 0 °C, the reaction mixture was diluted with AcOEt and filtrated through Celite®. The filtrate was evaporated and then purified by chromatography on silica gel (5 g) with 10% MeOH/DCM to afford **51a** (22.1 mg, 43%) as a light yellow solid.

2-cis-4-Aminocyclohexyl)-4H-benzo[h]chromen-4-one (51a). ^1H NMR (300 MHz, CDCl_3) δ 8.52-8.46 (1H, m, H-C(10)), 8.14 (1H, d, $J = 8.7$ Hz, H-C(5)), 7.95-7.92 (1H, m, H-C (7)), 7.76 (1H, d, $J = 8.7$ Hz, H-C(6)), 7.73-7.65 (2H, m, H-C(8, 9)), 6.41 (1H, s, H-C(3)), 3.26-3.15 (1H, m, H-C(1')), 2.84 (1H, tt, $J = 9.3, 4.3$ Hz), 2.19-2.08 (2H, m), 1.98-1.88 (2H, m). ^{13}C NMR (75 MHz, CDCl_3) δ 24.83 (2 Carbons), 32.58 (2 Carbons), 40.85, 46.21, 109.94, 119.93, 120.81, 122.22, 124.05, 124.99, 127.04, 128.17, 129.14, 135.86, 153.8, 171.37, 178.45. HRMS (ESI) calcd. for $\text{C}_{19}\text{H}_{20}\text{NO}_2$ $[\text{M} + \text{H}]^+$ 294.14940, found 294.15275.

2-trans-4-Aminocyclohexyl)-4H-benzo[h]chromen-4-one (51b). Yield: 63%, as a light yellow solid. ^1H NMR (300 MHz, CDCl_3) δ 8.52-8.44 (1H, m, H-C(10)), 8.14 (1H, d, $J = 8.7$ Hz, H-C(5)), 7.96-7.91 (1H, m, H-C (7)), 7.76 (1H, d, $J = 8.4$ Hz, H-C(6)), 7.74-7.65 (2H, m, H-C(8, 9)), 6.34 (1H, s, H-C(3)), 2.92-2.76 (1H, m, H-C(4')), 2.67 (1H, tt, $J = 12.1, 3.5$ Hz), 2.27-2.16 (2H, m), 2.13-2.02 (2H,

m), 1.76-1.60 (4H, m), 1.42-1.26 (2H, m). ^{13}C NMR (75 MHz, CDCl_3) δ 29.47 (2 Carbons), 35.43 (2 Carbons), 41.91, 50.04, 109.41, 119.98, 120.81, 122.16, 124.0, 125.0, 127.04, 128.17, 129.16, 135.86, 153.73, 171.48, 178.43. HRMS (ESI) calcd. for $\text{C}_{19}\text{H}_{20}\text{NO}_2$ $[\text{M} + \text{H}]^+$ 294.14940, found 294.15265.

2-(3-Aminocyclohexyl)-4H-benzo[h]chromen-4-one (51c). Yield: 80%, dr 3:1, as a light yellow solid. ^1H NMR (300 MHz, CDCl_3) δ 8.52–8.45 (1H, m, H-C(10)), 8.12 (1H, d, $J = 8.7$ Hz, H-C(5)), 7.96-7.89 (1H, m, H-C(7)), 7.75 (1H, d, $J = 8.8$ Hz, H-C(6)), 7.72-7.61 (2H, m, H-C(8, 9)), 6.35, 6.32 (3:1)(1H, s, H-C(3)), 4.52-4.35 (0.25H, m), 4.19-4.0 (0.25H), 3.50-3.38 (0.75H, m), 3.32-3.18(0.75H, m), 2.15-1.0 (10H, m). (major-isomer) ^{13}C NMR (75 MHz, CDCl_3) δ 19.83, 29.90, 33.15, 36.70, 37.39, 45.52, 109.78, 120.80, 122.20, 124.94, 127.01, 128.15, 129.11, 135.83, 153.78, 171.97, 178.44. (minor-isomer) ^{13}C NMR (75 MHz, CDCl_3) δ 22.64, 24.60, 36.01, 40.51, 41.91, 50.28, 109.37, 119.92, 121.75, 123.50, 124.03, 126.16, 127.86, 129.60, 137.50, 153.78, 171.18, 178.44. HRMS (ESI) calcd. for $\text{C}_{19}\text{H}_{20}\text{NO}_2$ $[\text{M} + \text{H}]^+$ 294.14940, found 294.14906.

4.2.9. General Procedure for Thioacetyl-containing Compounds 52a-c.

To a solution of **48b** (240 mg, 0.643 mmol) in DMF (3 mL) was added potassium carbonate (444 mg, 3.22 mmol) and thioacetic acid (229 μL , 3.22 mmol) at room temperature. After stirred for 13 h at 80 $^\circ\text{C}$, the reaction mixture was cooled to room temperature, and then quenched with ice water and diluted with 50% AcOEt/hexane. The organic layer was separated, washed with brine, dried over MgSO_4 , and evaporated. The residue was purified by MPLC (SNAP Ultra 10 g, 25 μm , 10 mL/min, 50% ether/hexane) to afford **52a** (80.5 mg, 35%) as a white powder, **52b** (65.2 mg, 28%) as a white powder and **50** (37.7 mg, 21%).

S-(cis-4-(4-oxo-4H-Benzo[h]chromen-2-yl)cyclohexyl) ethanethioate (52a). ^1H NMR (300 MHz, CDCl_3) δ 8.51-8.47 (1H, m, H-C(10)), 8.14 (1H, d, $J = 8.7$ Hz, H-C(5)), 7.96-7.93 (1H, m, H-C (7)), 7.77 (1H, d, $J = 8.6$ Hz, H-C(6)), 7.74-7.67 (2H, m, H-C(8, 9)), 6.36 (1H, s, H-C(3)), 4.07-4.02 (1H, m, C(4')), 2.79 (1H, tt, $J = 10.5, 3.6$ Hz, H-C(1')), 2.37 (3H, s, C(=O)-Me), 2.11-1.86 (8H, m). ^{13}C NMR (75 MHz, CDCl_3) δ 26.79 (2 carbons), 30.71 (2 Carbons), 30.99, 40.58, 41.48, 109.63, 119.98, 120.79, 122.14, 124.0, 125.05, 127.09, 128.19, 129.17, 135.87, 153.72, 171.0, 178.35, 195.12. HRMS (ESI) calcd. for $\text{C}_{21}\text{H}_{20}\text{O}_3\text{SNa}$ $[\text{M} + \text{Na}]^+$ 375.10308, found 375.10082.

S-(trans-4-(4-oxo-4H-Benzo[h]chromen-2-yl)cyclohexyl) ethanethioate (52b). ^1H NMR (300 MHz, CDCl_3) δ 8.51-8.47 (1H, m, H-C(10)), 8.13 (1H, d, $J = 8.7$ Hz, H-C(5)), 7.96-7.92 (1H, m, H-C (7)), 7.76 (1H, d, $J = 8.7$ Hz, H-C(6)), 7.74-7.67 (2H, m, H-C(8, 9)), 6.36 (1H, s, H-C(3)), 3.52 (1H, tt, $J = 12.4, 3.7$ Hz, C(4')), 2.79 (1H, tt, $J = 12.1, 3.2$ Hz, H-C(1')), 2.35 (3H, s, Me-C=O), 2.26-2.19 (4H, m), 1.91-1.78 (2H, m), 1.65-1.52 (2H, m). ^{13}C NMR (75 MHz, CDCl_3) δ 30.67 (3 Carbons), 30.79, 32.3 (2 Carbons), 41.31, 41.84, 109.54, 119.9, 120.74, 122.18, 123.95, 125.12, 127.14, 128.18, 129.26, 135.89, 153.78, 171.1, 178.44, 195.52. HRMS (ESI) calcd. for $\text{C}_{21}\text{H}_{21}\text{O}_3\text{S}$ $[\text{M} + \text{H}]^+$ 353.12114, found 353.12153.

S-(3-(4-oxo-4H-Benzo[h]chromen-2-yl)cyclohexyl) ethanethioate (52c). Yield. 64%, *cis:trans* = 2:1, as a white powder. ^1H NMR (300 MHz, CDCl_3) δ 8.52-8.43 (1H, m, H-C(10)), 8.13 (1H, d, J = 8.7 Hz, H-C(5)), 7.97-7.90 (1H, m, H-C(7)), 7.76 (1H, d, J = 8.8 Hz, H-C(6)), 7.74-7.66 (2H, m, H-C(8, 9)), 6.35, 6.33 (1:2)(1H, s, H-C(3)), 4.22-4.15 (0.4H, m, H-C(3')), 3.59 (0.6H, tt, J = 12.5, 3.8 Hz, H-C(3')), 3.04-2.83 (1H, m, H-C(1')), 2.05-2.41 (0.6H, m), 2.38, 2.34 (1:2)(3H, s, Me-C=O), 2.30-2.0 (2.6H, m), 1.94-1.81 (1.2H, m), 1.77-1.37 (3.6H, m). (*cis*-isomer) ^{13}C NMR (75 MHz, CDCl_3) δ 25.86, 29.54, 30.74, 32.16, 37.01, 41.35, 42.82, 109.52, 119.99, 120.78, 122.20, 123.97, 125.07, 127.10, 128.17, 129.19, 135.87, 153.70, 170.46, 178.34, 195.32. (*trans*-isomer) ^{13}C NMR (75 MHz, CDCl_3) δ 22.23, 30.15, 30.94, 30.99, 35.25, 38.92, 40.70, 109.77, 119.99, 120.80, 122.16, 123.97, 125.07, 127.10, 128.17, 129.19, 135.87, 153.70, 170.88, 178.34, 194.75. HRMS (ESI) calcd. for $\text{C}_{21}\text{H}_{21}\text{O}_3\text{S}$ $[\text{M} + \text{H}]^+$ 353.12114, found 353.12583.

4.2.10. General Procedure for Thiol-containing Compounds 53a-c.

To a solution of **52a** (35.7 mg, 0.101 mmol) in 50% THF/MeOH was added potassium carbonate (42.0 mg, 0.304 mmol) at room temperature. After being stirred for 45 min, the reaction mixture was cooled to 0 °C, and then neutralized with 1M HCl and diluted with DCM. The organic layer separated, washed with brine, dried over MgSO_4 , and evaporated. The residue was purified by chromatography on silica gel (5 g) with 1% MeOH/DCM to afford **53a** (18.4 mg, 59%) as a white powder.

2-(cis-4-Mercaptocyclohexyl)-4H-benzo[h]chromen-4-one (53a). ^1H NMR (300 MHz, CDCl_3) δ 8.54-8.50 (1H, m, H-C(10)), 8.14 (1H, d, J = 8.7 Hz, H-C(5)), 7.97-7.91 (1H, m, H-C(7)), 7.77 (1H, d, J = 8.7 Hz, H-C(6)), 7.75-7.65 (2H, m, H-C(8, 9)), 6.40 (1H, s, H-C(3)), 3.58-3.47 (1H, m, H-C(4')), 2.85-2.75 (1H, m, H-C(1')), 2.39-2.14 (2H, m), 2.10-1.88 (6H, m). ^{13}C NMR (75 MHz, CDCl_3) δ 24.97 (2 Carbons), 33.32 (2 Carbons), 35.72, 41.44, 109.84, 119.98, 120.82, 122.19, 124.04, 125.04, 127.11, 128.19, 129.17, 135.89, 153.78, 171.07, 178.43. HRMS (ESI) calcd. for $\text{C}_{19}\text{H}_{19}\text{O}_2\text{S}$ $[\text{M} + \text{H}]^+$ 311.11057, found 311.10689.

2-(trans-4-Mercaptocyclohexyl)-4H-benzo[h]chromen-4-one (53b). Yield: 65%, as a white powder. ^1H NMR (300 MHz, CDCl_3) δ 8.50-8.44 (1H, m, H-C(10)), 8.13 (1H, d, J = 8.7 Hz, H-C(5)), 7.96-7.91 (1H, m, H-C(7)), 7.76 (1H, d, J = 8.6 Hz, H-C(6)), 7.74-7.65 (2H, m, H-C(8, 9)), 6.33 (1H, s, H-C(3)), 2.95-2.81 (1H, m, H-C(4')), 2.72 (1H, tt, J = 11.7, 3.2 Hz, H-C(1')), 2.34-2.19 (4H, m), 1.79-1.49 (5H, m). ^{13}C NMR (75 MHz, CDCl_3) δ 30.96 (2 Carbons), 37.28 (2 Carbons), 37.44, 41.55, 109.47, 119.99, 120.80, 122.12, 123.98, 125.05, 127.06, 128.20, 129.19, 135.88, 153.71, 171.09, 178.37. HRMS (ESI) calcd. for $\text{C}_{19}\text{H}_{19}\text{O}_2\text{S}$ $[\text{M} + \text{H}]^+$ 311.11057, found 311.11211.

2-(3-Mercaptocyclohexyl)-4H-benzo[h]chromen-4-one (53c). Yield: 63%, *cis:trans* = 3:1, as a white powder. ^1H NMR (300 MHz, CDCl_3) δ 8.50-8.24 (1H, m, H-C(10)), 8.12 (1H, d, J = 8.7 Hz, H-C(5)), 7.95-7.89 (1H, m, H-C(7)), 7.74 (1H, d, J = 8.8 Hz, H-C(6)), 7.73-7.64 (2H, m, H-C(8, 9)), 6.35, 6.32 (1:3)(1H, s, H-C(3)), 3.72-3.62 (0.25H, m), 3.32 (0.25H, sep, J = 4.7 Hz), 3.01-2.87 (0.75H,

m), 2.74 (0.75H, dt, $J = 11.9, 4.0$ Hz), 2.55-2.45 (0.75H, m), 2.24-1.36 (9H, m). (*cis*-isomer) ^{13}C NMR (75 MHz, CDCl_3) δ 26.11, 29.30, 37.21, 37.52, 43.15, 109.48, 119.98, 120.75, 122.15, 123.97, 125.03, 127.07, 128.17, 129.20, 135.84, 153.68, 170.46, 178.34. (*trans*-isomer) ^{13}C NMR (75 MHz, CDCl_3) δ 20.31, 29.93, 33.66, 35.56, 36.89, 38.15, 109.84, 119.94, 120.76, 122.15, 123.95, 125.06, 127.08, 128.17, 129.20, 135.84, 153.74, 171.19, 178.34. HRMS (ESI) calcd. for $\text{C}_{19}\text{H}_{19}\text{O}_2\text{S}$ $[\text{M} + \text{H}]^+$ 311.11057, found 311.11132.

4.2.11. 4-(4-oxo-4H-Benzo[h]chromen-2-yl)cyclohexane-1-carbaldehyde (56).

To a solution of **41** (146 mg, 0.473 mmol) in DCM (5 mL) was added potassium carbonate (40.0 mg, 0.473 mmol) and Dess-Martin periodinate (402 mg, 0.946 mmol) at 0 °C. After being stirred for 1.5 h, the reaction mixture was diluted with DCM. The organic layer was separated, washed with brine, dried over MgSO_4 , and evaporated. The residue was purified by chromatography on silica gel (8 g) with 40% AcOEt/hexane to afford **56** (113 mg, 78%, dr 3:2) as a white powder. ^1H NMR (300 MHz, CDCl_3) δ 9.80, 9.72 (2:3)(1H, s, H-C=O), 8.50-8.41 (1H, m, H-C(10)), 8.14, 8.13 (2:3)(1H, d, $J = 8.7$ Hz, H-C(5)), 7.96-7.91 (1H, m, H-C(7)), 7.77, 7.75 (3:2)(1H, d, $J = 8.6$ Hz, H-C(6)), 7.73-7.64 (2H, m, H-C(8, 9)), 6.36, 6.32 (3:2)(1H, s, H-C(3)), 2.88-2.58 (1.4H, m), 2.46-2.21 (3.8H, m), 2.12-2.02 (0.8H, m), 1.88-1.63 (2.8H, m), 1.59-1.41 (1.2H, m). (major-isomer) ^{13}C NMR (75 MHz, CDCl_3) δ 25.47 (2 Carbons), 29.43 (2 Carbons), 42.09, 49.47, 109.48, 119.98, 120.78, 122.14, 123.96, 125.11, 127.09, 128.22, 129.23, 135.90, 153.73, 171.05, 178.43, 203.47. (minor-isomer) ^{13}C NMR (75 MHz, CDCl_3) δ 23.88 (2 Carbons), 27.06 (2 Carbons), 41.61, 46.24, 109.71, 119.93, 120.75, 122.11, 123.96, 125.07, 127.13, 128.16, 129.20, 135.87, 153.73, 170.95, 178.41, 204.37. HRMS (ESI) calcd. for $\text{C}_{20}\text{H}_{19}\text{O}_3$ $[\text{M} + \text{H}]^+$ 307.13342, found 307.13043.

4.2.12. 2-(trans-4-Ethynylcyclohexyl)-4H-benzo[h]chromen-4-one (57a, 57b).

To a solution of 1-diazoacetylphosphonic acid dimethyl ester (97.3 mg, 0.506 mmol) in MeOH (2 mL) was added potassium carbonate (70.0 mg, 0.675 mmol) and a solution of **56** (103 mg, 0.338 mmol) in MeOH (2 mL) at 0 °C. After being stirred for 4 h at room temperature, the reaction mixture was quenched with saturated NH_4Cl aqueous solution and diluted with DCM. The organic layer was separated, washed with brine, dried over MgSO_4 and evaporated. The residue was purified by MPLC (SNAP Ultra 10 g, 25 μm , 10 mL/min, 30% ether/hexane) to afford **57a** (11.0 mg, 11%) as a white powder and **57b** (73.7 mg, 72%) as a white powder.

2-(cis-4-Ethynylcyclohexyl)-4H-benzo[h]chromen-4-one (57a). ^1H NMR (300 MHz, CDCl_3) δ 8.54-8.47 (1H, m, H-C(10)), 8.14 (1H, d, $J = 8.7$ Hz, H-C(5)), 7.97-7.91 (1H, m, H-C(7)), 7.75 (1H, d, $J = 8.7$ Hz, H-C(6)), 7.74-7.64 (2H, m, H-C(8, 9)), 6.39 (1H, s, H-C(3)), 2.99-2.89 (1H, m, H-C(4')), 2.71 (1H, dt, $J = 11.4, 3.4$ Hz, H-C(1')), 2.19 (1H, d, $J = 2.5$ Hz, H-C \equiv C), 2.17-1.97 (6H, m), 1.78-1.64 (2H, m). ^{13}C NMR (75 MHz, CDCl_3) δ 25.93 (2 Carbons), 26.22, 30.11 (2 Carbons), 42.09, 70.25,

86.51, 109.48, 119.99, 120.83, 122.19, 124.06, 124.96, 127.02, 128.15, 129.12, 135.86, 153.74, 171.59, 178.49. HRMS (ESI) calcd. for $C_{21}H_{18}O_2Na$ $[M + Na]^+$ 325.12045, found 325.12143.

2-(trans-4-Ethynylcyclohexyl)-4H-benzo[h]chromen-4-one (57b). 1H NMR (300 MHz, $CDCl_3$) δ 8.50-8.44 (1H, m, H-C(10)), 8.13 (1H, d, $J = 8.7$ Hz, H-C(5)), 7.96-7.91 (1H, m, H-C(7)), 7.76 (1H, d, $J = 8.6$ Hz, H-C(6)), 7.74-7.65 (2H, m, H-C(8, 9)), 6.33 (1H, s, H-C(3)), 2.78-2.68 (1H, m), 2.45-2.35 (1H, m), 2.27-2.18 (4H, m), 2.12 (1H, d, $J = 2.3$ Hz, H-C \equiv C), 1.68-1.59 (4H, m). ^{13}C NMR (75 MHz, $CDCl_3$) δ 28.81, 29.8, 32.2, 41.69, 68.36, 87.75, 109.42, 119.98, 120.79, 122.13, 123.97, 125.01, 127.05, 128.18, 129.17, 135.85, 153.69, 171.25, 178.35. HRMS (ESI) calcd. for $C_{21}H_{18}O_2Na$ $[M + Na]^+$ 303.13850, found 325.12057.

4.2.13. General Procedure for Allene-containing Compounds (58a, 58b).

To a solution of **57a** (25.8 mg, 0.085 mmol) in dioxane (2 mL) was added paraformaldehyde (6.40 mg, 0.213 mmol), copper(I) iodide (8.13 mg, 0.043 mmol) and dicyclohexylamine (27.9 mg, 0.154 mmol) at room temperature. After being stirred for 30 min at reflux, the reaction mixture was cooled to room temperature, and then quenched with saturated NH_4Cl aqueous solution and diluted with DCM. The organic layer was separated, washed with brine, dried over $MgSO_4$, and evaporated. The residue was purified by flash chromatography on silica gel (10 g) with 1% MeOH/DCM to afford **58a** (9.50 mg 35%) as a yellow solid.

2-(cis-4-(Propa-1,2-dien-1-yl)cyclohexyl)-4H-benzo[h]chromen-4-one (58a). 1H NMR (300 MHz, $CDCl_3$) δ 8.51-8.46 (1H, m, H-C(10)), 8.14 (1H, d, $J = 8.7$ Hz), 7.96-7.91 (1H, m, H-C(7)), 7.76 (1H, d, $J = 8.8$ Hz, H-C(6)), 7.74-7.65 (2H, m, H-C(8, 9)), 6.38 (1H, s, H-C(3)), 5.16 (1H, q, $J = 6.7$ Hz, H-C=C), 4.80 (2H, dd, $J = 6.8, 4.3$ Hz, $H_2C=C$), 2.83 (1H, sep, $J = 4.5$ Hz, H-C(1')), 2.61-2.54 (1H, m, H-C(4')). ^{13}C NMR (75 MHz, $CDCl_3$) δ 26.09 (2 Carbons), 29.21 (2 Carbons), 32.37, 41.39, 76.21, 93.70, 109.77, 119.96, 120.85, 122.19, 124.94, 127.02, 128.18, 129.11, 135.87, 153.80, 171.81, 178.52. HRMS (ESI) calcd. for $C_{22}H_{20}O_2Na$ $[M + Na]^+$ 339.13610, found 339.13968.

2-(trans-4-(Propa-1,2-dien-1-yl)cyclohexyl)-4H-benzo[h]chromen-4-one (58b). Yield: 48%, as a yellow solid. 1H NMR (300 MHz, $CDCl_3$) δ 8.51-8.46 (1H, m, H-C(10)), 8.14 (1H, d, $J = 8.7$ Hz), 7.96-7.91 (1H, m, H-C(7)), 7.76 (1H, d, $J = 8.6$ Hz, H-C(6)), 7.74-7.64 (2H, m, H-C(8, 9)), 6.34 (1H, s, H-C(3)), 5.18 (1H, q, $J = 6.3$ Hz, H-C=C), 4.76 (2H, dd, $J = 6.6, 3.0$ Hz, $H_2C=C$), 2.68 (1H, tt, $J = 12.1, 3.5$ Hz), 2.27-2.19 (2H, m), 2.18-2.09 (1H, m), 2.08-2.0 (2H, m), 1.77-1.61 (2H, m), 1.42-1.26 (2H, m). ^{13}C NMR (75 MHz, $CDCl_3$) δ 30.41, 32.26 (2 Carbons), 36.09, 42.34, 76.05, 95.16, 109.33, 120.0, 120.84, 122.18, 124.04, 124.93, 127.0, 128.16, 129.11, 135.84, 153.73, 171.92, 178.48, 207.46. HRMS (ESI) calcd. for $C_{22}H_{21}O_2$ $[M + H]^+$ 317.15415, found 317.15246.

4.2.14. General Procedure for Azide-containing Compounds (59a, 59b).

To a solution of **46a** (38.5 mg, 0.134 mmol) in 50% THF/ H_2O (2 mL) was slowly added concentrated

hydrochloric acid (60 μ L) at 0 °C and allowed to stir for 15 min. The resulting solution was added sodium nitrite (13.8 mg, 0.201 mmol) and allowed to stir for 15 min at 0 °C. The reaction mixture was added sodium azide (11.3 mg, 0.172 mmol) at 0 °C and allowed to stir for 15 min at room temperature. The reaction mixture was then added ice water to yield a white precipitate. The slurry was purified by chromatography on silica gel (2 g) with 15% AcOEt/hexane to afford **59a** (40.1 mg, 95%) as a light yellow solid.

2-(4-Azidophenyl)-4H-benzo[h]chromen-4-one (59a). ^1H NMR (300 MHz, DMSO- d_6) δ 8.76-8.71 (1H, m, H-C(10)), 8.33 (2H, dt, $J = 8.9, 2.3$ Hz, H-Ar), 8.19-8.12 (1H, m, H-C(7)), 8.03 (1H, d, $J = 8.7$ Hz, H-C(5)), 7.98 (1H, d, $J = 8.7$ Hz, H-C(6)), 7.88-7.83 (2H, m, H-C(8,9)), 7.37 (2H, dt, $J = 8.9, 2.3$ Hz, H-Ar), 7.24 (1H, s, H-C(3)). ^{13}C NMR (75 MHz, DMSO- d_6) δ 108.30, 120.11, 120.46 (2 Carbons), 120.57, 122.88, 124.02, 126.03, 128.29, 128.33, 128.80 (2 Carbons), 128.87, 130.21, 131.12, 143.61, 153.0, 161.45, 177.70. HRMS (ESI) calcd. for $\text{C}_{19}\text{H}_{12}\text{N}_3\text{O}_2$ $[\text{M} + \text{H}]^+$ 314.09295, found 314.09538.

2-(3-Azidophenyl)-4H-benzo[h]chromen-4-one (59b). Yield: 91%, as a light yellow solid. ^1H NMR (300 MHz, DMSO- d_6) δ 8.72-8.67 (1H, m), 8.17-8.13 (1H, m), 8.12-8.07 (1H, m), 8.0 (2H, q, $J = 8.7$ Hz), 7.91 (1H, t, $J = 1.9$ Hz), 7.88-7.82 (2H, m), 7.67 (1H, d, $J = 8.0$ Hz), 7.45-7.4 (1H, m), 7.34 (1H, s, H-C(3)). ^{13}C NMR (75 MHz, DMSO- d_6) δ 109.36, 117.33, 120.11, 120.40, 122.67 (2 Carbons), 123.43, 123.89, 125.99, 128.24, 128.76, 130.12, 131.35, 133.46, 135.95, 141.06, 153.23, 161.31, 177.33. HRMS (ESI) calcd. for $\text{C}_{19}\text{H}_{11}\text{N}_3\text{O}_2\text{Na}$ $[\text{M} + \text{Na}]^+$ 336.07490, found 336.07702.

4.2.15. General Procedure for Phenol-containing Compounds (60a, 60b).

To a solution of **47a** (1.35 g, 4.48 mmol) in acetic acid (15 mL) was added 47% hydrogen bromide in water (15 mL) at room temperature. After being stirred for 2 h at 150 °C, the reaction mixture was cooled to room temperature, and then added ice water to yield a brown precipitate. The crude compound was purified by flash chromatography on silica gel (80 g) with 3% MeOH/DCM to afford **60a** (781 mg, 60%) as a white solid.

2-(4-Hydroxyphenyl)-4H-benzo[h]chromen-4-one (60a). ^1H NMR (300 MHz, DMSO- d_6) δ 10.34 (1H, m, H-O), 8.75-8.71 (1H, m, H-C(10)), 8.16-8.11 (3H, m), 8.02 (1H, d, $J = 8.7$ Hz, H-C(5)), 7.95 (1H, d, $J = 8.6$ Hz, H-C(6)), 7.87-7.82 (2H, m), 7.06 (1H, s, H-C(3)), 7.02-7.00 (2H, m).

2-(3-Hydroxyphenyl)-4H-benzo[h]chromen-4-one (60b). Yield: quant, as a white powder. ^1H NMR (300 MHz, DMSO- d_6) δ 9.96 (1H, br. s, H-O), 8.70-8.64 (1H, m, H-C(10)), 8.18-8.13 (1H, m, H-C(7)), 8.0 (2H, q, $J = 8.4$ Hz, H-C(5, 6)), 7.90-7.83 (2H, m, H-Ar), 7.69-7.65 (1H, m, H-Ar), 7.64 (1H, t, $J = 1.9$ Hz, H-Ar), 7.43 (1H, t, $J = 7.9$ Hz, H-Ar), 7.13 (1H, s, H-C(3)), 7.06-7.01 (1H, m, H-Ar).

4.2.16. General Procedure for O-carbamothioate-containing Compounds (61a, 61b).

To a solution of **60a** (79.5 mg, 0.278 mmol) in dry DMF (1 mL) was added sodium hydride (13.9

mg, 0.413 mmol) at 0 °C and allowed to stir for 15 min. The resulting mixture was added *N,N*-dimethylthiocarbamoyl chloride (51.3 mg, 0.414 mmol) and heated to 60 °C. After being stirred for 2 h, the reaction mixture was cooled to room temperature, and then added ice water and diluted with DCM. The organic layer was separated, washed with brine, dried over MgSO₄ and evaporated. The residue was purified by flash chromatography on silica gel (10 g) with 2% MeOH/DCM to afford **61a** (53.8 mg, 52%) as a white powder.

O-(4-(4-oxo-4H-Benzo[h]chromen-2-yl)phenyl) dimethylcarbamothioate (**61a**). ¹H NMR (300 MHz, CDCl₃) δ 8.67-8.61 (1H, m, H-C(10)), 8.20 (1H, d, *J* = 8.7 Hz, H-C(5)), 8.08 (2H, dt, *J* = 8.8, 2.4 Hz), 7.99-7.95 (1H, m, H-C (7)), 7.82 (1H, d, *J* = 8.7 Hz, H-C(6)), 7.76-7.71 (2H, m, H-C(8, 9)), 7.31 (2H, dt, *J* = 8.9, 2.3 Hz), 6.97 (1H, s, H-C(3)), 3.50, 3.41 (each, 3H, s, (Me)₂-N). ¹³C NMR (75 MHz, CDCl₃) δ 38.93, 43.39, 108.90, 120.28, 120.78, 122.37, 123.89 (2 Carbons), 124.14, 125.45, 127.24, 127.38 (2 Carbons), 128.30, 129.31, 129.63, 136.08, 153.58, 156.42, 162.03, 178.19, 187.04. HRMS (ESI) calcd. for C₂₂H₁₈NO₃S [M + H]⁺ 376.10074, found 376.09855.

O-(3-(4-oxo-4H-Benzo[h]chromen-2-yl)phenyl) dimethylcarbamothioate (**61b**). Yield: 31%, as a white powder. ¹H NMR (300 MHz, DMSO-*d*) δ 8.74-8.69 (1H, m, H-*Ar*), 8.20-8.13 (2H, m, H-*Ar*), 8.06-7.96 (3H, m, H-*Ar*), 7.89-7.83 (2H, m, H-*Ar*), 7.68 (1H, t, *J* = 8.0 Hz, H-*Ar*), 7.27 (1H, s, H-*Ar*), 3.42, 3.40 (each 3H, s, (Me)₂-N). ¹³C NMR (75 MHz, DMSO-*d*) δ 38.94, 43.45, 109.37, 120.33, 120.74, 120.86, 122.44, 123.73, 124.10, 125.51, 126.16, 127.26, 128.27, 129.33, 129.96, 133.25, 136.08, 153.56, 154.57, 161.76, 178.13, 187.32. HRMS (ESI) calcd. for C₂₂H₁₈NO₃ [M + H]⁺ 376.10074, found 376.10144.

4.2.17. General Procedure for S-carbamothioate-containing Compounds (**62a**, **62b**).

61a (53.8 mg, 0.144 mmol) was heated to 210 °C and allowed to stir for 8.5 h. The crude compound was purified by chromatography on silica gel (5 g) with 1% MeOH/DCM to afford **62a** (34.8 mg, 65%).

S-(4-(4-oxo-4H-Benzo[h]chromen-2-yl)phenyl) dimethylcarbamothioate (**62a**). ¹H NMR (300 MHz, CDCl₃) δ 8.66-8.60 (1H, m, H-C(10)), 8.19 (1H, d, *J* = 8.7 Hz, H-C(5)), 8.05 (2H, dt, *J* = 8.6, 2.0 Hz, H-*Ar*), 8.00-7.94 (1H, m, H-C (7)), 7.82 (1H, d, *J* = 8.5 Hz, H-C(6)), 7.77-7.70 (4H, m, H-*Ar*), 6.99 (1H, s, H-C(3)), 3.14, 3.08 (each, 3H, br. s, (Me)₂-N). ¹³C NMR (100 MHz, CDCl₃) δ 37.07, 37.147, 109.44, 120.83, 122.47, 124.24, 125.6, 126.64, 127.37 (2 Carbons), 128.38, 129.45, 132.6, 133.28, 136.15 (3 Carbons), 153.72, 162.14, 165.89, 178.31. HRMS (ESI) calcd. for C₂₂H₁₈NO₃S [M + H]⁺ 376.10074, found 376.09922.

S-(3-(4-oxo-4H-benzo[h]chromen-2-yl)phenyl) dimethylcarbamothioate (**62b**). Yield: 24%, as a brown powder. ¹H NMR (300 MHz, CDCl₃) δ 8.66-8.60 (1H, m, H-C(10)), 8.19 (1H, d, *J* = 8.7 Hz, H-C(5)), 8.16 (1H, t, *J* = 1.7 Hz), 7.99-7.95 (1H, m, H-C(7)), 7.82 (1H, d, *J* = 8.8 Hz, H-C(6)), 7.78-7.69 (3H, m), 7.63 (1H, d, *J* = 7.7 Hz), 6.99 (1H, s, H-C(3)), 3.22-3.02 (6H, m, (Me)₂-N). ¹³C NMR

(75 MHz, CDCl₃) δ 37.02, 109.33, 120.34, 120.76, 122.47, 124.13, 125.48, 126.86, 127.23, 128.27, 129.31, 129.65, 130.61, 132.81, 133.29, 136.08, 138.63, 153.60, 161.91, 166.0, 178.14. HRMS (ESI) calcd. for C₂₂H₁₈NO₃ [M + H]⁺ 376.10074, found 376.09873.

4.2.18. General Procedure for S-carbamothioate-containing Compounds (63a, 63b).

To a solution of **62a** (34.8 mg, 0.093 mmol) in MeOH (1 mL) was added 10% sodium hydroxide in MeOH (3 mL) at room temperature. After being stirred for 2h, the reaction mixture was neutralized with saturated NH₄Cl aqueous solution and diluted with DCM. The organic layer was separated, washed with brine, dried over MgSO₄ and evaporated. The residue was purified by chromatography on silica gel (5 g) with 1% MeOH/DCM to afford **63a** (14.0 mg, 50%) as a yellow powder.

2-(4-Mercaptophenyl)-4H-benzo[h]chromen-4-one (63a). ¹H NMR (300 MHz, CDCl₃) δ 8.64-8.59 (1H, m, H-C(10)), 8.19 (1H, d, *J* = 8.7 Hz, H-C(5)), 8.00-7.95 (1H, m, H-C (7)), 7.91 (2H, dt, *J* = 8.6, 2.2 Hz), 7.81 (1H, d, *J* = 8.8 Hz, H-C(6)), 7.77-7.70 (2H, m), 7.46 (2H, dt, *J* = 8.7, 2.2 Hz), 6.93 (1H, s, H-C(3)), 3.68 (1H, s, H-S). ¹³C NMR (75 MHz, CDCl₃) δ 108.29, 120.29, 120.77, 122.28, 124.09, 125.39, 126.76 (2Carbons), 127.19, 128.29, 128.96, 129.14 (2Carbons), 129.27, 136.04, 136.66, 153.45, 162.08, 178.15. HRMS (ESI) calcd. for C₁₉H₁₃O₃S [M + H]⁺ 305.06362, found 305.06375.

2-(3-Mercaptophenyl)-4H-benzo[h]chromen-4-one (63b). Yield: 53%, as a yellow powder. ¹H NMR (300 MHz, CDCl₃) δ 8.65-8.6 (1H, m, H-C(10)), 8.2 (1H, d, *J* = 8.7 Hz, H-C(8)), 7.98 (1H, q, *J* = 3.3 Hz), 7.95-7.93 (1H, m), 7.84-7.8 (2H, m), 7.78-7.72 (2H, m), 7.5-7.44 (2H, m), 6.95 (1H, s, H-C(3)), 3.68 (1H, s, H-S). ¹³C NMR (100 MHz, CDCl₃) δ 109.34, 120.40, 120.81, 122.43, 123.64, 124.16, 125.61, 126.75, 127.37, 128.39, 129.46, 129.94, 132.25, 132.83, 133.08, 136.16, 153.64, 161.90, 178.195. HRMS (ESI) calcd. for C₁₉H₁₃O₂S [M + H]⁺ 305.06362, found 305.05882.

4.3. EROD-assay

The recombinant human CYP1B1, 1A1, and 1A2 enzymes, each equipped with P450 reductase (Supersomes), were purchased from BD Biosciences. The reaction mixture was containing 100 mM potassium phosphate buffer (pH 7.4), 1.5 mM EDTA, 2 μ M 7-ethoxyresorufin, supersome, and various concentrations of compound in a total volume of 190 μ L. The concentration of CYP1B1, 1A1 and 1A2 was 6, 3, 6 nM, respectively. After pre-incubation at 37 °C for 5 min, the reactions were initiated by addition of 10 μ L of 50 mM NADPH. The time of incubation for system containing CYP1B1, 1A1 and 1A2 was 30, 15, 30 min, respectively. The formation of resorufin was determined fluorometrically (530 nm excitation and 590 nm emission) using F-7100 fluorescence spectrofluorometer (Hitach High-Tech Science, Tokyo, Japan). The IC₅₀ value for each compound was obtained by GraphPad Prism software.

4.4. Aqueous solubility

The aqueous solubility determination was based on saturation shake-flask method. The solvent was a solution in which PBS and ethanol were mixed at 9:1, and was added several mg of compound to make suspension in total volume 2 mL. The suspension was shaking at room temperature for overnight and then centrifuged at 15,000 \times g for 5 min. The supernatant was measured UV-absorbance, and the concentration of sample compound was calculated using a previously determined calibration curve which was corrected for the dilution factor of the sample.

4.5. Protein expression

4.5.1. Construction of the hCYP1B1 Expression Vector.

hCYP1B1 cDNA was amplified by PCR from Megaman human transcriptome library (Agilent Technologies, Inc). The forward primer sequence using for PCR are 5'-ATGGGCACCCAGCCTCAGCCC-3', and corresponding reverse primer sequence was 5'-TTGGCAAGTTTCCTTGGCTTGTA-3'. This full length hCYP1B1 cDNA was modified for expression in *Escherichia coli* and crystallization according to method previous reported by Wang et al.²⁸ The N-terminal 50 residues amino acid sequence was replaced with MAKKTSSKGK which is widely used in other microsomal P450 *Escherichia coli* expression system for improvement of solubility and stability.^{53,54} At C-terminus, 4 histidine tag was added to facilitate the purification of the expressed protein. The modified cDNA was inserted to pCW-LIC vector which was a gift from Cheryl Arrowsmith (Addgene plasmid # 26098) using with In-Fusion® Cloning System (Takara Bio, USA).

4.5.2. Protein expression

Expression of modified hCYP1B1 was conducted in co-expression system with chaperone protein of Gro ES and GroEL. Constructed expression vector for hCYP1B1 was transformed to competent cell

DH5 α which had previously transformed with pGro7 plasmid coding of GroES and GroEL (Takara Bio, Japan, Inc.). Transformants containing both the hCYP1B1 vector and pGro7 plasmid was selected by cultured at LB plate containing 100 μ g/ml ampicillin, and 20 μ g/ml chloramphenicol. Selected single colony was incubated in 10 mL of 2 \times YT medium containing both Amp and Cm at 37 $^{\circ}$ C for overnight. This saturated culture medium was seeded to 1 L of 2 \times YT medium with both antibiotics and cultured at 37 $^{\circ}$ C and 120 rpm until OD₆₀₀ of 0.6. Then, final concentration of 1 mM β -D-thiogalactoside for induction of hCYP1B1 expression, 4 mg/ml D-arabinose for induction of GroES/GroEL expression, 1 mM δ -aminolevulinic acid and 2.5 μ l/ml trace element solution (containing 27 mg/ml FeCl₃·6H₂O, 2 mg/ml ZnCl₂, 2 mg/ml CoCl₂·6H₂O, 2 mg/ml NaMoO₄·2H₂O, 1 mg/ml CaCl₂·2H₂O, 1 mg/ml CuCl₂, 0.5 mg/ml H₃BO₃, 0.1 ml/ml conc.HCl) for precursor of heme biosynthesis were added. The culture was incubated another 24 h at 27 $^{\circ}$ C, cells were harvested by centrifugation (7000 \times g for 5 min), suspended in 20 mL of lysozyme buffer (containing 100 mM Tris-HCl pH 8.0, 500 mM sucrose, 0.5 mM EDTA and 1 mg/ml lysozyme) at 4 $^{\circ}$ C for 1 h, and centrifuged again (7000 \times g for 20 min) to prepare spheroplast. This spheroplast was pooled and frozen at -78 $^{\circ}$ C prior to purification.

4.5.3. Protein purification

To purify for hCYP1B1 protein, the spheroplast was sonicated in 14 mL of lysis buffer (containing 50 mM Tris-HCl pH 8.0, 20% glycerol, 10 mM CHAPS, 300 mM NaCl, 1 mM TCEP, 0.5 mM EDTA, 1 mM PMSF) at 0 $^{\circ}$ C for 1 min \times 4 times. After centrifugation (20,000 \times g for 20 min), supernatant was applied to 1 ml of Ni-NTA beads equilibrated with wash buffer (containing lysis buffer component, excluding EDTA and PMSF) and washed with 5 mL of wash buffer, then eluted by 5 ml of elution buffer (containing 50 mM Tris-HCl pH 7.4, 20% glycerol, 10 mM CHAPS, 300 mM NaCl, 1 mM TCEP and 200 mM imidazole). The red eluate was conducted further purification: affinity column chromatography by 5 ml volume of HisTrap HP column (GE Healthcare), ion exchange purification using with 5 ml volume of HiTrap SP HP (GE Healthcare) and multiple gel filtration utilizing Supredex 200 Increase 10/300 (GE Healthcare) to obtain single peak fraction detected by 280 nm of absorbance. Apo form of hCYP1B1 was unstable and frequently precipitated, especially under condition with low ion strength, and high concentration at column top. Purified hCYP1B1 protein was identified as single band in SDS-PAGE at 55 kDa, and kept in crystallization buffer (containing 20 mM Tris-HCl pH 7.4, 20% glycerol, 10 mM CHAPS, 300 mM NaCl, 10 mM 2-mercaptoethanol). The concentration of hCYP1B1 was measured by changes in absorbance due to binding between carbon monoxide and ferrous heme reduced by sodium hydrosulfite.^{55,56}

4.6. Spectroscopic analysis

All spectra were recorded using V-630 spectrophotometer (Jasco, Tokyo, Japan) at room temperature. The concentration of hCYP1B1 was 1 μ M diluted with ABS buffer (containing 100 mM potassium phosphate, 20% glycerol, 0.5% sodium cholate, 1 mM EDTA and 0.4% tween 20). The total volume of measured solution was 1 ml in plastic cuvette. Absolute spectra in the 300 to 700 nm region were obtained by subtracting value of blank cuvette containing ABS buffer from value of sample cuvette containing P450 and ABS buffer. In the case of measuring ferrous heme, sodium hydrosulfite was added to both cuvettes to the concentration of 1 mM. Absorbances with inhibitor were measured by adding inhibitor in DMSO to each cuvette. The different spectrum with various concentrations of inhibitor was recorded in the 350 to 500 nm region. In this case, the sample cuvette was added inhibitor in DMSO, on the other hand, corresponding blank cuvette was added the same volume of DMSO as inhibitor. Spectral dissociation constant (Ks) were calculated from the titration curve of the difference in absorbance between the peak and trough vs the inhibitor concentration using GraphPad Prism software (GraphPad Software).

4.7. X-ray Crystallographic Analysis.

A mixture of 200 μ M CYP1B1 in buffer containing 20 mM Tris-HCl pH 7.4, 20% glycerol, 10 mM CHAPS, 300 mM NaCl, 10 mM 2-mercaptoethanol and compound **49a** (5 equiv) was incubated at room temperature for 1 h. The mixture of **49a**/CYP1B1 was crystallized by hanging drop vapor diffusion using a series of precipitant solutions containing 0.1 M HEPES (pH 6.8-7.5), 5-15% (w/v) PEG8k, and 10-30% ethylene glycol. Droplets for crystallization were prepared by mixing 1 μ L of complex solution and 1 μ L of precipitant solution, and were equilibrated against 300 μ L of precipitant solution at 25 °C. The mixture was stored at 25 °C, and crystals appeared after a week. Prior to diffraction data collection, crystals were soaked in a LVCO-1 (LV Cryo Oil) (MiTeGen, NY, U.S.). Diffraction data sets of **49a**/CYP1B1 complex were collected at 100 K in a stream of nitrogen gas at beamlines NW12A of KEK-PFAR (Tsukuba, Japan). Reflections were recorded with an oscillation range per image of 1.0°. Diffraction data were indexed, integrated, and scaled using the program iMOSFLM^{57,58} in the CCP4 program.⁵⁹ The structures of ternary complex were solved by molecular replacement with the software Phaser⁶⁰ in the Phenix program⁶¹ using hCYP1B1 coordinates (PDB code 3PM0), and finalized sets of atomic coordinates were obtained after iterative rounds of model modification with the program Coot⁶² and refinement with refmac5.⁶³⁻⁶⁷

4.8. Docking Analysis.

Docking studies were performed using the Surflex Dock program on SYBYL X2 software, and the X-ray structures of CYP1B1 (PDB: 3PM0) and CYP1A1 (PDB: 4I8V). The orientation of CD-ring in **49a** was restricted to conformation in crystal structure. A reasonable model having common points among the top 20 conformation calculated was chosen.

Declaration of interest

Conflicts of interest: none

Acknowledgements

This work was financially supported by the Platform for Drug Discovery, Informatics, and Structural Life Science from the Japan Agency for Medical Research and Development (AMED), and was also supported by the MEXT-Supported Program for the Strategic Research Foundation at Private Universities (2013–2017). Synchrotron radiation experiments were performed at the Photon Factory (Proposal No. 2017G588), and we are grateful for the assistance provided by the beamline scientists at the Photon Factory.

References and notes

1. Nebert DW, Russell DW. Clinical importance of the cytochromes P450. *Lancet*. 2002;360(9340):1155-1162. doi:10.1016/S0140-6736(02)11203-7
2. Meunier B, Visser P De, Shaik S. Mechanism of Oxidation Reactions Catalyzed by Cytochrome P450 Enzymes. 2004.
3. Guengerich FP. Cytochrome P450 and Chemical Toxicology Cytochrome P450 and Chemical Toxicology. *Chem Res Toxicol*. 2008;21(Table 1):70-83. doi:10.1021/tx700079z
4. Zanger UM, Schwab M. Cytochrome P450 enzymes in drug metabolism: Regulation of gene expression, enzyme activities, and impact of genetic variation. *Pharmacol Ther*. 2013;138(1):103-141. doi:10.1016/j.pharmthera.2012.12.007
5. Liu J, Sridhar J, Foroozesh M. Cytochrome P450 family 1 inhibitors and structure-activity relationships. *Molecules*. 2013;18(12):14470-14495. doi:10.3390/molecules181214470
6. Cui J, Li S. Inhibitors and Prodrugs Targeting CYP1 : A Novel Approach in Cancer Prevention and Therapy. 2014:519-552.
7. Dutour R, Poirier D. Inhibitors of cytochrome P450 (CYP) 1B1. *Eur J Med Chem*. 2017;135:296-306. doi:10.1016/j.ejmech.2017.04.042
8. Nelson DR. The cytochrome p450 homepage. *Hum Genomics*. 2009;4(1):59-65. <http://www.ncbi.nlm.nih.gov/pubmed/19951895>. Accessed October 25, 2018.
9. Conney AH. Induction of microsomal enzymes by foreign chemicals and carcinogenesis by polycyclic aromatic hydrocarbons: G.H.A.Clowes memorial lecture. *Cancer Res*. 1982;42(DECEMBER):4875-4917.
10. Shimada T, Hayes CL, Yamazaki H, et al. Activation of Chemically Diverse Procarcinogens P-450 IBI1 by Human Cytochrome. *City*. 1996:2979-2984. doi:10.1016/0041-008X(89)90251-2
11. Kim JH, Stansbury KH, Walker NJ, Trush MA, Strickland PT, Sutter TR. Metabolism of benzo[a]pyrene and benzo[a]pyrene-7,8-diol by human cytochrome P450 1B1. *Carcinogenesis*.

- 1998;19(10):1847-1853. doi:10.1093/carcin/19.10.1847
12. Androutsopoulos VP, Tsatsakis AM, Spandidos DA. Cytochrome P450 CYP1A1: Wider roles in cancer progression and prevention. *BMC Cancer*. 2009;9:1-17. doi:10.1186/1471-2407-9-187
 13. Spink DC, Eugster H-P, Lincoln DW, et al. 17 β -Estradiol hydroxylation catalyzed by human cytochrome P450 1A1: A comparison of the activities induced by 2,3,7,8-tetrachlorodibenzo-p-dioxin in MCF-7 cells with those from heterologous expression of the cDNA. *Arch Biochem Biophys*. 1992;293(2):342-348. doi:10.1016/0003-9861(92)90404-K
 14. Hayes CL, Spink DC, Spink BC, Cao JQ, Walker NJ, Sutter TR. 17 beta-estradiol hydroxylation catalyzed by human cytochrome P450 1B1. *Proc Natl Acad Sci U S A*. 1996;93(18):9776-9781. doi:10.1073/pnas.93.18.9776
 15. Yamazaki H, Shaw PM, Guengerich FP, Shimada T. Roles of cytochromes P450 1A2 and 3A4 in the oxidation of estradiol and estrone in human liver microsomes. *Chem Res Toxicol*. 1998;11(6):659-665. doi:10.1021/tx970217f
 16. Pike MC, Krailo MD, Henderson BE, Casagrande JT, Hoel DG. "Hormonal" risk factors, "breast tissue age" and the age-incidence of breast cancer. *Nature*. 1983;303(5920):767-770. doi:10.1038/303767a0
 17. Schütze N, Vollmer G, Tiemann I, Geiger M, Knuppen R. Catecholestrogens are MCF-7 cell estrogen receptor agonists. *J Steroid Biochem Mol Biol*. 1993;46(6):781-789. <http://www.ncbi.nlm.nih.gov/pubmed/8274412>. Accessed August 23, 2018.
 18. Emons G, Merriam GR, Pfeiffer D, Loriaux DL, Ball P, Knuppen R. Metabolism of exogenous 4- and 2-hydroxyestradiol in the human male. *J Steroid Biochem*. 1987;28(5):499-504. doi:10.1016/0022-4731(87)90508-5
 19. Lee AJ, Cai MX, Thomas PE, Conney AH, Zhu BT. Characterization of the oxidative metabolites of 17 β -estradiol and estrone formed by 15 selectively expressed human cytochrome P450 isoforms. *Endocrinology*. 2003;144(8):3382-3398. doi:10.1210/en.2003-0192
 20. Van Aswegen CH, Purdy RH, Wittliff JL. Binding of 2-hydroxyestradiol and 4-hydroxyestradiol to estrogen receptors from human breast cancers. *J Steroid Biochem*. 1989;32(4):485-492. <http://www.ncbi.nlm.nih.gov/pubmed/2542691>. Accessed August 23, 2018.
 21. Cavalieri EL, Stack DE, Devanesan PD, et al. Molecular origin of cancer: catechol estrogen-3,4-quinones as endogenous tumor initiators. *Proc Natl Acad Sci U S A*. 1997;94(20):10937-10942. doi:10.1073/pnas.94.20.10937
 22. Chakravarti D, Mailander PC, Li KM, et al. Evidence that a burst of DNA depurination in SENCAR mouse skin induces error-prone repair and forms mutations in the H-ras gene. *Oncogene*. 2001;20(55):7945-7953. doi:10.1038/sj.onc.1204969
 23. McKay a, Greenlee F, Murray GI, Taylor MC, Burke MD, Melvin WT. Tumor-specific Expression of Cytochrome P450 CYP1B1 CYP1B1. *Cell*. 1997;44(0):3026-3031.

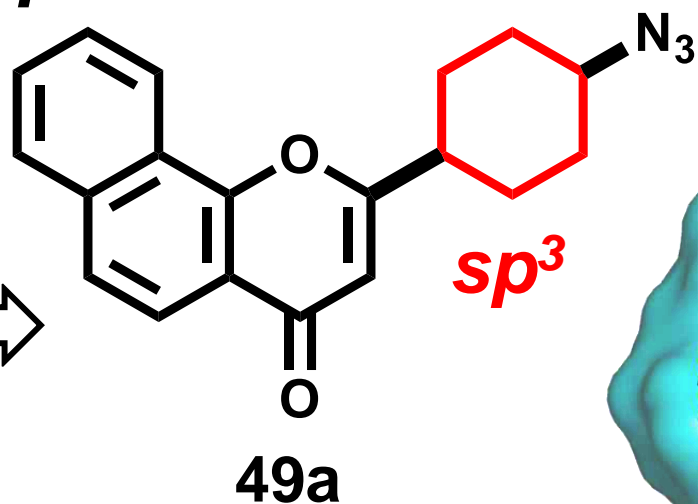
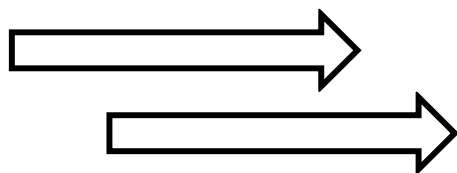
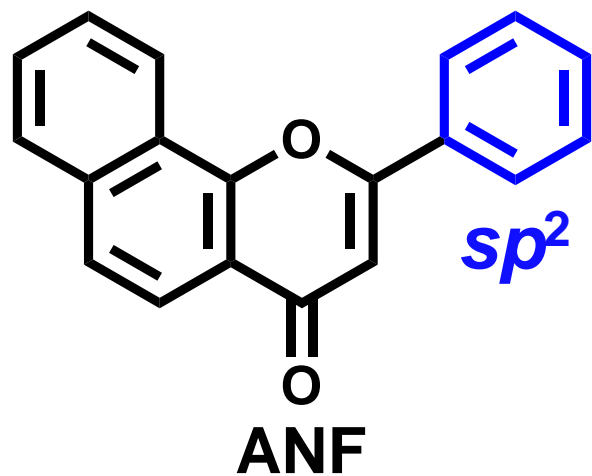
24. Liehr JG, Ricci MJ. 4-Hydroxylation of estrogens as marker of human mammary tumors. *Proc Natl Acad Sci U S A*. 1996;93(8):3294-3296. doi:10.1073/pnas.93.8.3294
25. McFadyen MC, McLeod HL, Jackson FC, Melvin WT, Doehmer J, Murray GI. Cytochrome P450 CYP1B1 protein expression: a novel mechanism of anticancer drug resistance. *Biochem Pharmacol*. 2001;62(2):207-212. doi:http://dx.doi.org/10.1016/S0006-2952(01)00643-8
26. Cazzaniga M, Bonanni B, Dai X, et al. METABOLISM OF TAMOXIFEN BY RECOMBINANT HUMAN CYTOCHROME P450 ENZYMES : FORMATION OF THE 4-HYDROXY, 4- α -HYDROXY AND N- DESMETHYL METABOLITES AND ISOMERIZATION OF trans -4-HYDROXYTAMOXIFEN ABSTRACT : *J Cancer*. 2002;7(13):869-874. doi:10.1016/j.steroids.2007.07.009.New
27. Rochat B, Morsman JM, Murray GI, Figg WD, McLeod HL. Human CYP1B1 and anticancer agent metabolism: mechanism for tumor-specific drug inactivation? *J Pharmacol Exp Ther*. 2001;296(2):537-541.
28. Wang A, Savas U, Stout CD, Johnson EF. Structural characterization of the complex between alpha-naphthoflavone and human cytochrome P450 1B1. *J Biol Chem*. 2011;286(7):5736-5743. doi:10.1074/jbc.M110.204420
29. Walsh AA, Szklarz GD, Scott EE. Human cytochrome P450 1A1 structure and utility in understanding drug and xenobiotic metabolism. *J Biol Chem*. 2013;288(18):12932-12943. doi:10.1074/jbc.M113.452953
30. Sansen S, Yano JK, Reynald RL, et al. Adaptations for the oxidation of polycyclic aromatic hydrocarbons exhibited by the structure of human P450 1A2. *J Biol Chem*. 2007;282(19):14348-14355. doi:10.1074/jbc.M611692200
31. Jain AN. Surflex-Dock 2.1: Robust performance from ligand energetic modeling, ring flexibility, and knowledge-based search. *J Comput Aided Mol Des*. 2007;21(5):281-306. doi:10.1007/s10822-007-9114-2
32. Cui J, Meng Q, Zhang X, Cui Q, Zhou W, Li S. Design and Synthesis of New α -Naphthoflavones as Cytochrome P450 (CYP) 1B1 Inhibitors To Overcome Docetaxel-Resistance Associated with CYP1B1 Overexpression. *J Med Chem*. 2015;450:150401151839001. doi:10.1021/acs.jmedchem.5b00265
33. Ishikawa M, Hashimoto Y. Improvement in aqueous solubility in small molecule drug discovery programs by disruption of molecular planarity and symmetry. *J Med Chem*. 2011;54(6):1539-1554. doi:10.1021/jm101356p
34. Savjani KT, Gajjar AK, Savjani JK. Drug Solubility: Importance and Enhancement Techniques. *ISRN Pharm*. 2012;2012(100 mL):1-10. doi:10.5402/2012/195727
35. Nomura S, Endo-Umeda K, Fujii S, Makishima M, Hashimoto Y, Ishikawa M. Structural development of tetrachlorophthalimides as liver X receptor β (LXR β)-selective agonists with

- improved aqueous solubility. *Bioorganic Med Chem Lett*. 2018;28(4):796-801.
doi:10.1016/j.bmcl.2017.12.024
36. Fujita Y, Yonehara M, Tetsuhashi M, Noguchi-Yachide T, Hashimoto Y, Ishikawa M. β -Naphthoflavone analogs as potent and soluble aryl hydrocarbon receptor agonists: Improvement of solubility by disruption of molecular planarity. *Bioorganic Med Chem*. 2010;18(3):1194-1203. doi:10.1016/j.bmc.2009.12.036
37. Lovering F. Escape from Flatland 2: Complexity and promiscuity. *Medchemcomm*. 2013;4(3):515-519. doi:10.1039/c2md20347b
38. Lovering F, Bikker J, Humblet C. Escape from flatland: Increasing saturation as an approach to improving clinical success. *J Med Chem*. 2009;52(21):6752-6756. doi:10.1021/jm901241e
39. Baker W. 322. Molecular rearrangement of some o-acyloxyacetophenones and the mechanism of the production of 3-acylchromones. *J Chem Soc*. 1933;0(0):1381. doi:10.1039/jr9330001381
40. Mahal HS, Venkataraman K. 387. Synthetical experiments in the chromone group. Part XIV. The action of sodamide on 1-acyloxy-2-acetonaphthones. *J Chem Soc*. 1934;0(0):1767. doi:10.1039/jr9340001767
41. Lim J, Choi J, Kim HS, et al. Synthesis of Terminal Allenes via a Copper-Catalyzed Decarboxylative Coupling Reaction of Alkynyl Carboxylic Acids. *J Org Chem*. 2016;81(1):303-308. doi:10.1021/acs.joc.5b02361
42. Burke DM, Mayer RT. Ethoxyresorufin: Microsomal Preferentially Direct Which Assay Is of O-Dealkylation By 3-Methylcholanthrene. *Drug Metab Dispos*. 1974;2(6):583-588.
43. Dutour R, Roy J, Cortés-Benítez F, Maltais R, Poirier D. Targeting Cytochrome P450 (CYP) 1B1 Enzyme with Four Series of A-Ring Substituted Estrane Derivatives: Design, Synthesis, Inhibitory Activity, and Selectivity. *J Med Chem*. 2018;450:acs.jmedchem.8b00907. doi:10.1021/acs.jmedchem.8b00907
44. Avdeef A, Testa B. Physicochemical profiling in drug research: A brief survey of the state-of-the-art of experimental techniques. *Cell Mol Life Sci*. 2002;59(10):1681-1689. doi:10.1007/PL00012496
45. Isin EM, Guengerich FP. Substrate binding to cytochromes P450. *Anal Bioanal Chem*. 2008;392(6):1019-1030. doi:10.1007/s00216-008-2244-0
46. Imai Y, Hashimoto-yutsudo C, Satake H, Girardin A, Sato R. Multiple forms of cytochrome P-450 purified from liver microsomes of phenobarbital- and 3-methylcholanthrene-pretreated rabbits: I. resolution, purification, and molecular properties. *J Biochem*. 1980;88(2):489-503. doi:10.1093/oxfordjournals.jbchem.a132996
47. Mailman RB, P KA, Baker RC, Hodgson E. Effect of chemical structure on type II spectra in mouse hepatic microsomes. *Drug Metab Dispos*. 1974;2(3):301-308.
48. Schenkman OB, Cinti DL, Orrenius S, Moldeus P, Kraschnitz R. The Nature of the Reverse Type

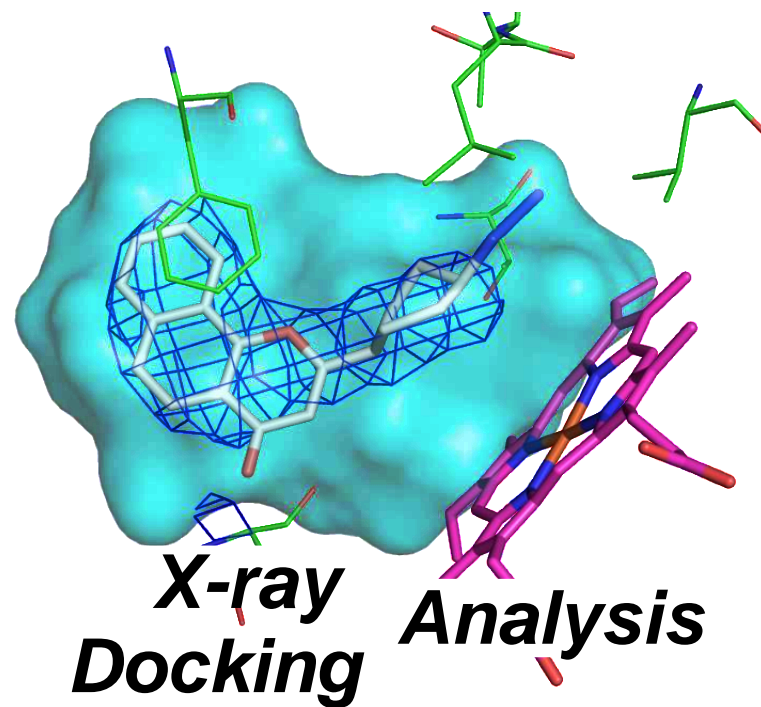
- I (Modified Type II) Spectral Change in Liver Microsomes. *Biochemistry*. 1972;11(23):4243-4251. doi:10.1021/bi00773a008
49. Sono M, Andersson LA, Dawson JH. Sulfur Donor Ligand Binding to Ferric Cytochrome P-450-CAM and. *J Biol Chem*. 1982;257(14):8308-8320.
50. Sevrioukova IF, Poulos TL. Pyridine-substituted desoxyritonavir is a more potent inhibitor of cytochrome P450 3A4 than ritonavir. *J Med Chem*. 2013;56(9):3733-3741. doi:10.1021/jm400288z
51. Tu Y, Deshmukh R, Sivaneri M, Szklarz GD. Application of molecular modeling for prediction of substrate specificity in cytochrome P450 1A2 mutants. *Drug Metab Dispos*. 2008;36(11):2371-2380. doi:10.1124/dmd.108.022640
52. Nishida CR, Everett S, Ortiz de Montellano PR. Specificity Determinants of CYP1B1 Estradiol Hydroxylation. *Mol Pharmacol*. 2013;84(3):451-458. doi:10.1124/mol.113.087700
53. Wester MR, Johnson EF, Marques-Soares C, et al. Structure of mammalian cytochrome P450 2C5 complexed with diclofenac at 2.1 Å resolution: Evidence for an induced fit model of substrate binding. *Biochemistry*. 2003;42(31):9335-9345. doi:10.1021/bi034556l
54. Arase M, Waterman MR, Kagawa N. Purification and characterization of bovine steroid 21-hydroxylase (P450c21) efficiently expressed in Escherichia coli. *Biochem Biophys Res Commun*. 2006;344(1):400-405. doi:10.1016/j.bbrc.2006.03.067
55. Omura, Tsuneo; Sato R. The Carbon Monoxide-binding pigment of Liver Microsomes. *J Biol Chem*. 1964;239(7):2370-2378.
56. Guengerich FP, Martin M V, Sohl CD, Cheng Q. Measurement of cytochrome P450 and NADPH-cytochrome P450 reductase. *Nat Protoc*. 2009;4(9):1245-1251. doi:10.1038/nprot.2009.121
57. Leslie AGW, Powell HR. Processing diffraction data with mosflm. In: Springer, Dordrecht; 2007:41-51. doi:10.1007/978-1-4020-6316-9_4
58. Battye TGG, Kontogiannis L, Johnson O, Powell HR, Leslie AGW. *iMOSFLM* : a new graphical interface for diffraction-image processing with *MOSFLM*. *Acta Crystallogr Sect D Biol Crystallogr*. 2011;67(4):271-281. doi:10.1107/S0907444910048675
59. Collaborative Computational Project, Number 4. The CCP4 suite: programs for protein crystallography. *Acta Crystallogr Sect D Biol Crystallogr*. 1994;50(5):760-763. doi:10.1107/S0907444994003112
60. Bunkóczi G, Echols N, McCoy AJ, et al. *Phaser.MRage* : automated molecular replacement. *Acta Crystallogr Sect D Biol Crystallogr*. 2013;69(11):2276-2286. doi:10.1107/S0907444913022750
61. Adams PD, Afonine P V., Bunkóczi G, et al. *PHENIX* : a comprehensive Python-based system for macromolecular structure solution. *Acta Crystallogr Sect D Biol Crystallogr*. 2010;66(2):213-221. doi:10.1107/S0907444909052925

62. Emsley P, Lohkamp B, Scott WG, Cowtan K. Features and development of *Coot*. *Acta Crystallogr Sect D Biol Crystallogr*. 2010;66(4):486-501. doi:10.1107/S0907444910007493
63. Murshudov GN, Skubák P, Lebedev AA, et al. *REFMAC 5* for the refinement of macromolecular crystal structures. *Acta Crystallogr Sect D Biol Crystallogr*. 2011;67(4):355-367. doi:10.1107/S0907444911001314
64. Steiner RA, Lebedev AA, Murshudov GN, IUCr. Fisher's information in maximum-likelihood macromolecular crystallographic refinement. *Acta Crystallogr Sect D Biol Crystallogr*. 2003;59(12):2114-2124. doi:10.1107/S0907444903018675
65. Winn MD, Isupov MN, Murshudov GN. Use of TLS parameters to model anisotropic displacements in macromolecular refinement. *Acta Crystallogr D Biol Crystallogr*. 2001;57(Pt 1):122-133. <http://www.ncbi.nlm.nih.gov/pubmed/11134934>. Accessed November 7, 2018.
66. Pannu NS, Murshudov GN, Dodson EJ, Read RJ. Incorporation of prior phase information strengthens maximum-likelihood structure refinement. *Acta Crystallogr D Biol Crystallogr*. 1998;54(Pt 6 Pt 2):1285-1294. <http://www.ncbi.nlm.nih.gov/pubmed/10089505>. Accessed November 7, 2018.
67. Murshudov GN, Vagin AA, Dodson EJ, IUCr. Refinement of Macromolecular Structures by the Maximum-Likelihood Method. *Acta Crystallogr Sect D Biol Crystallogr*. 1997;53(3):240-255. doi:10.1107/S0907444996012255

Dearomatization and Optimization



Complex structure 49a/CYP1B1



Inhibitory Potency 
Selectivity 
Solubility 

CYP1B1 IC_{50} = 4.4 nM
CYP1A1 IC_{50} = 525 nM
CYP1A2 IC_{50} = 667 nM